MICROWAVE SPECTRA, MOLECULAR STRUCTURE, QUADRUPOLE COUPLING, DIPOLE MOMENT, AND RING BENDING VIBRATION OF 1, 3, 2-DIOXABOROLANE

Thesis for the Degree of Ph. D. MICHIGAN STATE UNIVERSITY

James Henry Hand

1965



This is to certify that the

thesis entitled

MICROWAVE SPECTRA, MOLECULAR STRUCTURE, QUADRUPOLE COUPLING, DIPOLE MOMENT, AND RING BENDING VIBRATION OF 1,3,2-DIOXABOROLANE

presented by

James Henry Hand

has been accepted towards fulfillment of the requirements for

Ph.D degree in Chemistry

Major professor

Date November 9, 1965

		:
		•
		ţ
		1
		}
		•
		,
		i
		,
		

ABSTRACT

MICROWAVE SPECTRA, MOLECULAR STRUCTURE, QUADRUPOLE COUPLING, DIPOLE MOMENT, AND RING BENDING VIBRATION OF 1,3,2-DIOXABOROLANE

by James Henry Hand

A brief history of microwave spectroscopy is presented. The theory of rotational spectra, with emphasis on the method of molecular structure determination and on vibration-rotation interaction, is discussed. The microwave spectrometer is described.

The observed excited vibrational states have been assigned to the first two excited states of a symmetric ring bending vibration. The excited vibrational energy levels are estimated to lie 53 and $88~\rm cm^{-1}$ above the ground state for QCH₂CH₂OPH and 22 and $66~\rm cm^{-1}$ above the

ground state for OCD_2CD_2OBH . The vibrational effects which have been observed are consistent with a double minimum potential with a small central barrier.

A suggested method for calculating the energies of centrifugal distortion is included.

MICROWAVE SPECTRA, MOLECULAR STRUCTURE, QUADRUPOLE COUPLING, DIPOLE MOMENT, AND RING BENDING VIBRATION OF 1,3,2-DIOXABOROLANE

Ву

James Henry Hand

A THESIS

Submitted to
Michigan State University
in partial fulfillment of the requirements
for the degree of

DOCTOR OF PHILOSOPHY

Department of Chemistry

1965

DEDICATION

To the future for David and Kristin

ACKNOWLEDGMENTS

It is a sincere pleasure to thank Dr. Richard H. Schwendeman for the generous guidance and intellectual stimulation which he provided during the course of this research.

Financial aid in the form of fellowships from the National Science Foundation and Petroleum Research Fund is gratefully acknowledged.

Dr. Sheldon G. Shore deserves thankful recognition for his interest in and initial suggestion of research on this compound, for his gift of some of the chemical samples, and for his aid in preparing the remaining samples.

TABLE OF CONTENTS

			Pa ge
I	HIST	ORICAL BACKGROUND AND AN INTRODUCTION	1
II	THEO	RETICAL BASIS OF ROTATIONAL SPECTROSCOPY	7
	2.1	Introduction	7
	2.2	Rigid Rotor Model	7
		A) Moments of Inertia and Principal Axes B) Quantum Mechanical Treatment of Rigid Rotation	7 10
	2.3	Perturbations to the Rigid Rotor	20
		A) Stark Effect	20 21
	2.4	Determining a Molecular Structure	24
	2.5	The Coupling of Vibration and Rotation	27
III	DESC	RIPTION OF THE MICROWAVE SPECTROMETER	36
	3.1	Introduction	. 36
	3.2	Klystron Oscillators	36
	3.3	Waveguide Absorption Cell	40
	3.4	Square Wave Stark Modulation	40
	3.5	Detection System	41
	3.6	Frequency Measurements	. 42
IV	MICR	OWAVE STUDIES ON 1,3,2-DIOXABOROLANE	46
	4.1	Introduction	46
	4.2	Preparation of The Chemical Samples	46
	4.3	Examination of the Rotational Spectra	52
	4.4	Discussion of the Bond Characters	64

TABLE OF CONTENTS (Cont.)

																								Page
	4.5		ermi truo			n 0	f i	the •	Mc	1e •	cu •	1a •	r •	Sy •	mn •	et •	ry •	, a	nd •	l •	•			70
		A) B) C) D)	Int Det	lati ten s term	ity ina	, M iti	eas on	of	eme tt	ent 1e	s Di	ро	1e	: N	Ion	ne r	nt	•	•					7 1 73 78
		2,		itru					•	•	•	•	•	•	•	•	•	•	•	•	•	•	•	83
	4.6	Int	erpi	reta	tic	n	of	th	e F	Rin	g	Ве	nd	lir	ng	Vi	br	at	ic	n				89
	4.7	Dis	cuss	sion	ı .		•		•		•			•		•	•	•	•	•	•	•		96
V	CENT	RIFU	GAL	DIS	TOF	RTI	ON	CA	LCI	JLA	TI	ON	S		•	•	•	•		•	•			99
	BIBL	IOGR	APH	<i>.</i>	•					•		•		•				•		•	•	•	•	106
	APPE:	NDIC	ES		•									•	•					•			•	109
		Α	COM	PUTE	RF	PRO	GRA	M	"E]	GV	ΆL	S"		•		•	•	•	•	•				110
		В	KRA] SU	TCH JBST				E E(QU <i>P</i>	TI.	ON.	s •	FC	R •	TH.	ΙΕ •	4-	-D						112

LIST OF TABLES

TABLE		P a ge
I	Klystrons, frequency meters, and crystal detectors now in use at Michigan State University	. 3 9
II	Initial structural parameters assumed for 1,3,2-dioxaborolane	. 53
III	Observed and calculated frequency splitting of quadrupole hyperfine components for 1,3,2-dioxaborolane: parent species	. 56
IV	Experimental hypothetical unsplit frequencies assigned for 1,3,2-dioxaborolane: parent species	. 57
V	Observed and calculated frequency splittings of quadrupole hyperfine components for 1,3,2-dioxaborolane: 4,4,5,5-tetradeutero - species	60
VI	Experimental hypothetical unsplit frequencies assigned for 1,3,2-dioxaborolane: 4,4,5,5-tetradeutero-species	. 61
VII	Observed and calculated frequency splittings of quadrupole hyperfine components for 1,3,2-dioxaborolane: 13C species	- . 63
VIII	Experimental hypothetical unsplit frequencies assigned for 1,3,2-dioxaborolane: ¹³ C species	. 63
IX	Observed and calculated frequency splitting of quadrupole hyperfine components and experimental hypothetical unsplit frequencies assigned for 1,3,2-dioxaborolane: 10B species	. 65
X	Rotational constants, principal moments of inertia, and second moments of inertia for 1,3,2-dioxaborolane	. 66
XI	Quadrupole coupling constants for 1,3,2-dioxaborolane	. 67
XII	Relative intensity of the $(2_{12} \rightarrow 3_{03})$ to the $(2_{02} \rightarrow 3_{13})$ transitions in 1,3,2-dioxaborolane .	. 75
XIII	Relative intensity of the $(3_{03} \rightarrow 4_{14})$ to the $(3_{13} \rightarrow 4_{04})$ transitions in tetradeutero-1,3,2-dioxaborolane	• 77

LIST OF TABLES (Cont.)

TABLE		P a ge
XIV	Relative intensities of rotational transitions and estimated vibrational energies	77
VX	Data used in the dipole moment calculations	81
XVI	Calculated dipole moment components	82
XVII	Principal axis coordinates of the atoms in OCH2CH2OBH	86
XVIII	Structural parameters calculated for 1,3,2-dioxa-borolane	87
XIX	Values of <0 > determined from the model for the vibrational motion	95

LIST OF ILLUSTRATIONS

Figure		Pa	a ge
1	Block diagram of the microwave spectrometer	•	37
2	Stark waveguide cross section	•	40
3	Detection preamplifier input circuit	•	42
4	Projection of 1,2,3-dioxaborolane in its principal ab and ac planes	•	88

I. HISTORICAL BACKGROUND AND AN INTRODUCTION

The microwave region of the electromagnetic spectrum lies between the far-infrared and radio-frequency regions. It includes the wavelengths between .05 and 30 centimeters, corresponding to energies of 20 to .033 cm⁻¹. The energies involved in microwave spectroscopy are generally expressed in megacycles/second (Mc/sec.), with 1 Mc/sec. = 10^6 cycles/sec., approximately 3 x 10^{-5} cm⁻¹.

The first spectroscopic experiments in the microwave region were performed by Cleeton and Williams (1) in 1933 on the ammonia molecule. This intense and profuse spectrum arises from the inversion motion of NH₃. However, in subsequent experiments on other molecules the observed spectra were of rotational transitions, and today the microwave region is considered the domain of rotational spectroscopy. Other experimentation at that time was limited by the spectrometer sensitivity and associated technological problems. These were greatly abated by advances made in developing the 1.25 centimeter radar system. After the Second World War much surplus radar equipment became available to universities, stimulating a wide range of experimentation. Advances were then made in microwave spectroscopy which may be classified as instrumental advances to high resolution, high precision, and high sensitivity, and theoretical and conceptual advances.

The first high-resolution experiments were performed by Bleaney and Penrose (2), on the NH₃ spectrum, and by Coles and Good (3), also on the NH₃ spectrum. The latter workers observed hyperfine splittings which were later demonstrated to be caused by (and prove the existence

of) the ¹⁴N nuclear quadrupole moment (4). A second type of hyperfine effect is due to internal rotation in which case the observed splitting provides a sensitive method for calculating the height of the potential barrier to internal rotation. The first of many barrier height determinations was made by Burkhard and Dennison (5) on methy1 alcohol. With the treatments of Herschbach and others (6) microwave spectroscopy is now the most accurate method for determining the potential energy constants for small barriers. High barriers and conformational isomers are also easily studied, since each excited torsional state and each distinct conformation gives rise to a separate rotational spectrum which can be resolved and separately studied.

With present spectrometers, resolution of splittings of 0.5 Mc/sec. is almost routine. Therefore observation of hyperfine effects is generally the rule rather than the exception.

The high precision possible for microwave measurements was demonstrated by Dakin, Good, and Coles (7) in 1947. They measured the $J = 1 \rightarrow 2$ transition of OCS at 24325 Mc/sec. with an uncertainty of \pm 0.02 Mc/sec., less than 1 part per million. This precision is now generally attained, and may be surpassed in special cases.

The sensitivity of a microwave spectrometer was greatly increased as the result of a suggestion by Hughes and Wilson (8). They showed that applying a periodic electric field to the absorption cell would produce a molecular Stark effect, modulating the absorption transitions. This permitted the use of tuned and lock-in amplifiers in the detection circuit. Transitions with absorption coefficients as low as $10^{-10}/\mathrm{cm}$, have been observed, but $10^{-9}/\mathrm{cm}$, is a more common lower limit of detectability.

The Stark effect also provides a convenient method for measuring molecular dipole moments. Debye (9) predicted that in an electric field, splitting of rotational transitions should occur and should be proportional to the square of the dipole moment and the square of the electric field strength. Dakin, Good, and Coles first demonstrated this to be true for OCS. Precise measurements of the dipole moment of OCS (10) have provided a secondary standard on which dipole moment measurements may be based.

The increase in sensitivity of the spectrometer resulting from use of the Stark effect permitted experiments to be performed on molecules with less intense spectra. Many linear and symmetric top molecules were then studied, due to the simplicity of their spectra. Asymmetric top molecules were considered later, when improved methods for calculating their energy levels had been developed, and when the quantum-mechanical treatments had been extended to permit calculation of perturbation and hyperfine effects, (and when there were no more simple symmetric tops to study).

The determination of molecular structures is the most widely recognized use of microwave spectroscopy. The internuclear (bond) distances and angles were at one time determined by varying them systematically to reproduce the moments of inertia calculated from the rotational constants. Later, least squares fittings to the moments of intertia of several isotopic species were made. Kraitchman (11) suggested an improved method for determining the nuclear coordinates from differences between the moments of inertia of the normal species and those of isotopically-substituted species. Costain (12) later

showed that better results, giving less variation with the isotopic species used, were obtained by this "substitution" method. This method is rather insensitive to atoms located near a principal inertial plane but is highly sensitive to the effects of vibrations of these atoms. No simple relationship between substitution coordinates obtained by the Kraitchman-Costain method and equilibrium values has yet been established. Presently a prohibitively large amount of experimental data is needed to obtain an equilibrium structure. These include knowledge of the vibration-rotation coupling constants for each singly excited vibrational state for each isotopic species, or complete knowledge of the quartic and cubic potential constants for each vibrational mode. It is therefore not surprising that the determination of a substitution structure is accepted as a pragmatistic experimental goal.

Direct observations of vibrational effects on rotational spectra have also been made, in which pure rotational transitions for molecules in excited vibrational states have been observed. One example of this is the study by Chan, Zinn, Fernandez, and Gwinn (13) on the four-membered ring trimethylene oxide. They observed rotational spectra at room temperature for the ground state and four excited vibrational states of a ring puckering vibration. From intensity measurements and far-infrared data they estimated the first vibrational state to be about 70 cm⁻¹ above the ground state. They also found that the A and C rotational constants increased in a zig-zag pattern with increasing vibrational energy. This non-linear increase could be explained only by a double minimum potential function for an out-of-plane

vibration. A further discussion of their work, and similar results for other ring compounds is included with the results of the present study.

The experimental work reported in this thesis deals with the microwave spectrum of 1,3,2-dioxaborolane. The existence of this compound was first reported by Schlesinger and Burg (14) in 1942. Recently Rose and Shore (15) at The Ohio State University have refined the preparation procedure and have extensively investigated its physical and chemical properties. They report the vapor phase to be essentially monomeric and highly stable at -78°. The disproportionation reaction in the vapor phase

 $\frac{\text{QCH}_2\text{CH}_2\text{OBH}}{\text{C}}(g) \iff \frac{1}{6} \text{B}_2\text{H}_6(g) + \frac{1}{3} (\text{CH}_2\text{O})_2\text{BOCH}_2\text{CH}_2\text{OB}(\text{OCH}_2)_2(s)$ has an equilibrium constant at 25° of $\text{K}_{\text{Eq}}^{25} = 25 \pm 3$. At room temperature the condensed phase is a tacky or viscous liquid which has a great tendency to change to a non-volatile glassy solid. The liquid may be regenerated by careful warming to about 40° .

Dr. R. H. Schwendeman of Michigan State University began the study of the microwave spectrum of 1,3,2-dioxaborolane for several reasons. One was that the value of the dipole moment was of great interest to the Ohio State chemists; also there was his general interest in microwave studies of small ring compounds, with the added stimulus of the uniqueness of this small boron heterocycle having sufficient vapor pressure at -780 to permit its gas phase spectrum to be examined.

Dr. Schwendeman found that 1,3,2-dioxaborolane was a suitable and interesting subject for microwave spectroscopic experimentation.

The spectrum was fairly intense and he estimated the dipole moment to

be about 2 Debyes. He observed rotational transitions for the ground vibrational state and similar transitions for an excited vibrational state. The relative intensity of this second set of transitions indicated that the vibrational level involved must be quite low to be so highly populated at dry ice temperature. It also seemed that the effects of nuclear spin statistics on the relative intensities were present. His hypothesis was that the effects of a ring deformation vibration were being observed, this being the most reasonable type of low-frequency vibration which might be expected.

The present study was then undertaken to learn more about 1,3,2-dioxaborolane in general and about the vibrational effects in particular.

In presenting the methods, results, and conclusions of this study, a general theoretical background to rotational spectroscopy will first be discussed. Next the spectrometer which was used will be described. Then the methods used to analyze the rotational spectrum and the basic results of the analysis will be presented. Finally, a model system for the vibrational effects will be considered, and the observed effects and their implications will be discussed in light of results on similar molecules.

The final chapter in this thesis presents the results of a study concerning the problem of the calculation of the effects of centrifugal distortion on rotational spectra.

II. THEORETICAL BASIS OF ROTATIONAL SPECTROSCOPY

2.1 Introduction

Molecular rotational spectroscopy is most conveniently considered in terms of the angular momentum properties of a model rigid rotor. This approximate description of a molecule predicts the major features of its rotational spectrum. The effects of an electric field (Stark effect), a quadrupolar nucleus, and vibrational motions, can then be treated as perturbations to the rigid rotor results.

The theory of the rigid rotor is presented first, including a discussion of moments of inertia and principal axes, and a quantum mechanical treatment for symmetric and then for asymmetric top molecules. The second section introduces the perturbation results for the Stark effect and for nuclear quadrupole coupling. The third section is a discussion of how a molecular structure may be determined from the frequencies of rotational transitions. Finally, a theoretical approach to vibration-rotation coupling is presented, along with some implications of this coupling for the determination of molecular co-ordinates. The consideration of vibrational effects is continued in Chapter IV in order that the theory for each of several perturbations might be presented at the time the vibrational effects which were observed in the rotational spectrum are reported.

2.2 Rigid Rotor Model

A) Moments of Inertia and Principal Axes

In the rigid rotor model a molecule is considered to be a

rigid body composed of n point-masses with the entire mass of each atom concentrated at its nuclear position. If an arbitrary cartesian coordinate system is established, each mass $\mathbf{m_i}$ at a distance $\mathbf{r_i'}$ from the origin has coordinates $\mathbf{x_i'}$, $\mathbf{y_i'}$, $\mathbf{z_i'}$. The moment of inertia about the α axis is then defined as

$$I_{\alpha\alpha} = \sum_{i=1}^{n} m_{i}(\beta_{i}^{2} + \gamma_{i}^{2}), \quad \alpha \neq \beta \neq \gamma = x',y',z'.$$
 (2-1)

The product of inertia $I_{\alpha\beta}$ for $\alpha \neq \beta$ is defined as

$$I_{\alpha\beta} = -\sum_{i=1}^{n} m_i \alpha_i \beta_i. \qquad (2-2)$$

To shift the arbitrary coordinate system to a center of mass system, the parallel axis theorem may be applied. To apply this theorem, the coordinates of the center of mass in the original system, x_0,y_0,z_0 , must be established by applying the center of mass conditions to obtain

$$\alpha_0 = \frac{1}{M} \sum_{i=1}^{n} m_i \alpha_i$$
 etc., where $M = \sum_i m_i$. (2-3)

Then by the parallel axis theorem

$$I_{\alpha} = I_{\alpha}' - M(\beta_0^2 + \gamma_0^2), \text{ and}$$

$$I_{\alpha\beta} = I_{\alpha\beta}' - M(\alpha_0\beta_0).$$
(2-4)

Alternatively, the location vector $\overrightarrow{r_i}$ of each atom in the center-of-mass system is related to its original vector $\overrightarrow{r_i}$ by the vector $\overrightarrow{r_0}$ as $\overrightarrow{r_i} = \overrightarrow{r_i} - \overrightarrow{r_0}$ where $\overrightarrow{r_0} = x_0 \overrightarrow{i} + y_0 \overrightarrow{j} + z_0 \overrightarrow{k}$. Then the moment of inertia tensor or dyadic I may be written in a dyadic notation for the center-of-mass system as

$$I = \sum_{i} m_{i} (r_{i}^{2} \overline{1}^{2} - \overline{r}_{i}^{2} \cdot \overline{r}_{i}^{2})$$
 (2-5)

where $\overline{1}$ is the unit dyadic.

A tensor P, the second moment tensor, is defined by

$$P = \sum_{i} m_{i} \overline{r}_{i}^{} \overline{r}_{i}^{}$$

and may be represented as

$$P = \begin{bmatrix} P_{xx} & P_{xy} & P_{xz} \\ P_{yx} & P_{yy} & P_{yz} \\ P_{zx} & P_{zy} & P_{zz} \end{bmatrix}, \qquad (2-6)$$

with elements of the form

$$P_{xx} = \sum_{i} m_{i} x_{i}^{2},$$

$$P_{xy} = P_{yx} = \sum_{i} m_{i} x_{i} y_{i}.$$
(2-7)

If points proportioned to the values of $I^{-1/2}$ are plotted in a Cartesian coordinate system which has its origin at the center of mass and its axes identical to those about which $I^{-1/2}$ was evaluated, the surface which is described is designated the momental ellipsoid. The principal axes of this ellipsoid are the "principal axes of inertia" or simply principal axes. In practice the principal axes of a molecule are located by rotating an arbitrary center-of-mass axis system until the products of inertia vanish.

The moment of inertia tensor may be regarded formally as a symmetric matrix. Therefore diagonalizing I' by the similarity transformation SI'S = I is equivalent to rotating the arbitrary axis system to the principal axis system. The same transformation

diagonalizes P, since P commutes with I. The eigenvalues of I and P are related by the equations

$$I_{\alpha} = P_{\beta\beta} + P_{\gamma\gamma}$$
, etc., (2-8)

and

$$P_{\alpha\alpha} = \frac{1}{2}[I_{\beta} + I_{\gamma} - I_{\alpha}], \text{ etc.}$$
 (2-9)

The procedures for locating the principal axes may be simplified for molecules which possess elements of symmetry. The following rules may be used to determine principal axes by inspection:

- A plane of symmetry contains two of the principal axes and is perpendicular to the third.
- 2) A two-fold axis of symmetry is a principal axis.
- 3) A three-fold or higher axis of symmetry is a principal axis and the other two axes are any two mutually perpendicular axes which pass through the center of mass and are perpendicular to the symmetry axis.

The utility of principal axes and the dependence of a rotational spectrum on the principal moments of inertia are discussed in the following section. The determination of molecular coordinates from observed moments of inertia is discussed in section 2.4.

B) Quantum Mechanical Treatment of Rigid Rotation

The quantum mechanical treatment of rigid rotation utilizes the Hamiltonian operator,

$$H = \frac{\pi}{2} \left[\frac{P^2}{I_x} + \frac{P^2}{I_y} + \frac{P^2}{I_z} \right], \qquad (2-10)$$

where P_x^2 , P_y^2 , P_z^2 are operators corresponding to the square of the

projection of the total angular momentum along the x, y, z molecule-fixed principal axes, and I_x , I_y , I_z are the principal moments of inertia.

The angular momentum operators are defined by the commutation relations,

$$P_{x}P_{z} - P_{z}P_{x} = (P_{x}, P_{z}) = -iP_{z}$$

$$(P_{y}, P_{z}) = -iP_{x}$$

$$(P_{z}, P_{x}) = -iP_{y}.$$
(2-11)

From (2-11) it may be shown that the operator for the square of the total angular momentum P^2 commutes with the square of each of the three components; that is, if

$$P^2 = P_X^2 + P_Y^2 + P_Z^2$$
, then (2-12)

$$(P^2, P_X^2) = (P^2, P_Y^2) = (P^2, P_Z^2) = 0.$$
 (2-13)

Combining the convention for designating the experimentally observed moments of inertia as I_a , I_b , I_c with the requirement that $I_a \leq I_b \leq I_c$, a molecule may be classified as shown below.

Name	Requirement
Spherical top	$I_a = I_b = I_c$
Symmetric top	
Linear	$I_a = 0$, $I_b = I_c$
Prolate	$I_a + I_b = I_c$
Ob la te	$I_a = I_b + I_c$
Asymmetric top	$I_a \neq I_b \neq I_c$

In discussing symmetric and asymmetric tops the question of how to identify the x, y, z axes with the a, b, c principal axes arises. The six possibilities are

	Ir	ı1	II ^r	II ¹	IIIr	III ¹
x <->	b	С	С	а	a	b
y <- >	С	b	a	С	b	a
z <->	a	a	b	b	С	С

The following discussion will assume an oblate top and axis identification ${\rm III}^1$; to obtain the corresponding expressions for a prolate top it is necessary only to interchange a and c and also interchange ${\rm K}_{-1}$ and ${\rm K}_{-1}$. This will correspond to axis identification ${\rm I}^{\rm r}$.

Symmetric Top. - For the case with two equal moments of inertia in (2-10) the Schrödinger wave equation may be solved in closed form. The resulting eigenfunctions and eigenvalues are labeled by three quantum numbers, J, K, M,

 $J = 0,1,2, \cdots$

where $J(J + 1)\hbar^2$ is the square of the total angular momentum of the molecule,

 $K = 0, \pm 1, \pm 2, \cdots, \pm J$

where Kh is the projection of the total angular momentum along the molecule-fixed z axis, and

 $M = O, \pm 1, \pm 2, \cdots, \pm J$

where Mh is the projection of the total angular momentum along the space fixed Z axis.

The eigenfunctions Ψ JKM satisfy the operator equations

$$P^{2} \Psi_{JKM} = J(J + 1) \hbar^{2} \Psi_{JKM},$$

$$P_{Z} \Psi_{JKM} = K \hbar \Psi_{JKM}, \text{ and} \qquad (2-14)$$

$$P_{Z} \Psi_{JKM} = M \hbar \Psi_{JKM}.$$

Matrix elements in the ψ JKM basis set may be constructed for the operators in equations (2-11). The non-zero elements are

where

$$< K|P_{x}|K> = for J = J', M = M',$$

and

$$<$$
 J,K,M|P_x|J',K',M'> = $\int \psi_{J,K,M}^* P_x \psi_{J',K',M'} d\tau$.

The arbitrary phase factor has been chosen to make P_y real positive and P_x imaginary.

The eigenvalues for free rotation corresponding to the $\psi_{\rm JKM}$ eigenfunctions depend only on J and K, and the rotational constants B and C as

$$W_{JK} = h[B(J)(J + 1) + (C - B)K^2]$$
 (2-16)

where
$$B = \frac{h}{8\pi^2 I_b}$$
, $C = \frac{h}{8\pi^2 I_c}$.

Asymmetric Top. - The rigid asymmetric rotor problem has no general closed-form solution. It is best treated in a matrix formulation; fortunately the matrices encountered may be factored into direct sums of finite matrices. Consequently, the numerical problem of diagonalization is well-suited to high speed digital computers.

Since the symmetric top eigenfunctions form a complete orthogonal set when an infinite number are taken, a suitable combination of them may be used as a basis set to solve the rigid asymmetric rotor problem to as high a degree of accuracy as desired. The total angular momentum operator P^2 commutes with the asymmetric rotor Hamiltonian, as does P_Z , but P_Z does not. Thus J and M are still "good" quantum numbers but K no longer is.

The Hamiltonian in matrix form may be represented as

$$H = A P^2 + B P^2 + C P^2$$
 (2-17)

where P_z^2 , etc. indicate the matrices whose elements are given in (2-15). The desired eigenvalues are the elements of the matrix W obtained by reducing H to diagonal form (diagonalizing H). This is accomplished by the similarity transformation

$$\widetilde{T} \quad H \quad T = W$$
(2-18)

The task of diagonalizing the whole Hamiltonian is greatly simplified by three properties of ${\tt H}$.

(1) Since there are no non-zero matrix elements listed in (2-15) which connect levels of different J or M, the entire matrix is diagonal in J and may be separated into a block for each J and M. Each block will be of dimension 2J + 1 corresponding to the possible

values of K. Note that this also permits a finite number of symmetric rotor eigenfunctions to be used as the basis set for asymmetric rotator functions of a given J.

(2) Since \underline{H} has elements only of the type $\langle K | K \rangle$ and $\langle K | K \pm 2 \rangle$, none of the elements of odd K are connected to elements of even K and the blocks may be further factored. A unitary transformation due to Wang (16), $\widetilde{X} \, \underline{H} \, \underline{X} = \underline{H}'$, accomplishes this. Here \underline{H}' is the Hamiltonian in the "Wang symmetric rotor basis". A block of X has the form

$$\frac{1}{\sqrt{2}} \qquad \begin{bmatrix}
+1 & 0 & 0 & 0 & +1 \\
0 & +1 & 0 & +1 & 0 \\
0 & 0 & \sqrt{2} & 0 & 0 \\
0 & +1 & 0 & -1 & 0 \\
+1 & 0 & 0 & 0 & -1
\end{bmatrix}$$

This transformation is equivalent to taking linear combinations of the basis functions as

The Wang transformation factors each J block into four sub-blocks labeled E^+ , O^+ , O^- , E^- since each contains only elements of odd or even K and the symmetric (+) or antisymmetric (-) combination of the wave functions.

(3) The Hamiltonian may be recast to a "reduced energy" form by assuming a general linear transformation of the variables A, B, C as

$$A' = \sigma A + \rho,$$

$$B^{\dagger} = \sigma B + \rho,$$

$$C' = \sigma C + \rho.$$
(2-19)

(Note that the operators P_a^2 , P_b^2 , P_c^2 do not depend on this scaling of A, B, C.) The rigid rotor Hamiltonian in terms of the primed constants is

$$H (A', B', C') = A' P_a^2 + B' P_b^2 + C' P_c^2$$
.

Substituting from (2-19)

$$H(A',B',C') = [(\sigma A + \rho)P_a^2 + (\sigma B + \rho)P_b^2 + (\sigma C + \rho)P_c^2].$$
 (2-20)

Collecting terms in σ and ρ

$$H(A',B',C') = \sigma(AP_a^2 + BP_b^2 + CP_c^2) + \rho[P_a^2 + P_b^2 + P_c^2]$$

$$= \sigma H(A,B,C) + \rho P^2. \qquad (2-21)$$

Thus the original Hamiltonian H (A,B,C) may be written as

$$H = H'/\sigma - \rho/\sigma P^2$$
. (2-22)

Of the many possible choices for $\,\sigma,\,\,\rho\,\,$ two very useful ones are those of Ray (17) and Wang

Ray Wang
$$\sigma = \frac{2}{(A-C)} \qquad \sigma = \frac{2}{(2C-B-A)}$$

$$\rho = -\frac{(A+C)}{(A-C)} \qquad \rho = -\frac{(A+B)}{(2C-B-A)}$$

$$A' = 1 \qquad A' = \frac{A-B}{2C-B-A} = b_0$$

$$B' = \frac{2B-A-C}{A-C} \stackrel{\text{!`}}{=} X \qquad B' = \frac{B-A}{2C-B-A} = -b_0$$

$$C' = -1 \qquad C' = 1 .$$

In both cases it is seen that H(A',B',C') is a function of one variable, determined only by the relative sizes of A, B, C. Thus the eigenvalues of H' are "reduced" energies, functions of the asymmetry parameter K or b_0 .

The matrix result of this transformation assuming either of the symmetric rotator bases described above is that $P/\sigma J(J+1)E$, a constant times the unit matrix, is subtracted from the diagonal of each J block and a second constant, σ , is factored from the remaining matrix block.

The total matrix result may be written as

$$\widetilde{W} = \widetilde{T} H(A,B,C)T$$

$$= \widetilde{T} \widetilde{X} \left[\frac{H'}{G} - \frac{\rho}{G} P^2 \right] X T = \frac{1}{G} \widetilde{T} \widetilde{X} H' X T - \frac{\rho}{G} \widetilde{T} \widetilde{X} P^2 X T \qquad (2-23)$$

and since $\widetilde{T} \widetilde{X} P^2 X T = J(J + 1)E$, \widetilde{W} is diagonal when $\widetilde{T} \widetilde{X} H' X T$ is diagonal.

The rigid rotor energy may be written as

$$W_r/h = \frac{A+C}{2} J(J+1) + \frac{A-C}{2} E_{\tau}^J(\dot{\gamma}(), \text{ or } W_r/h = \frac{A+B}{2} J(J+1) + \frac{2C-B-A}{2} w_{\tau}^J(b_0)$$

where E_{τ}^{J} (%) and w_{τ}^{J} (b₀) are the reduced energy eigenvalues of

$$H' = P_a^2 - P_c^2 + \chi P_b^2 \quad \text{and}$$

$$H' = P_c^2 - b_0 \left[P_b^2 - P_a^2\right] \quad \text{respectively, and are}$$
(2-25)

calculated by numerical methods.

The original utility of the reduced energy transformation was that tables of reduced energies needed to be prepared at intervals of only one parameter, the asymmetry parameter. Entries for an arbitrary value of the asymmetry parameter could be obtained by interpolation.

The availability of computers has eliminated the use of tables for most work, but the reduced energy method still has advantages for these calculations.

Partial derivatives of the energy levels with respect to the rotational constants, for equations such as

$$dW_{r} = \frac{1}{h} \left[\frac{\partial W_{r}}{\partial A} dA + \frac{\partial W_{r}}{\partial B} dB + \frac{\partial W_{r}}{\partial C} dC \right], \qquad (2-26)$$

may be calculated at the same time that the energy levels are computed. These derivatives are just the diagonal values of P_a^2 , P_b^2 , P_c^2 calculated in the same basis set as the energy, i.e. the diagonal values of $T \times P_a^2 \times T$ etc. where T was the matrix which diagonalized the Hamiltonian. These derivatives are used, as will be shown later, in calculating the nuclear quadrupole coupling energies and in deducing rotational constants from an observed spectrum.

For the asymmetric rotor, K is not a proper quantum number so it is necessary to label the eigenfunctions and energy levels with another quantum number. The easiest way is to number the energy levels in each J block in order of increasing energy; the symbol $_{\rm T}$ is used and assumes the integer values from -J to +J . A second, more useful way depends on the energy limits which are approached as the asymmetry tends toward each of the symmetric rotor limits. As $^{\times}$ -> -1, the prolate symmetric rotor limit, the calculated energies approach those of the prolate symmetric rotor. Similarly as $^{\times}$ -> +1, the oblate symmetric rotor limit, the calculated energies approach those of the oblate symmetric rotor. Thus each asymmetric rotor energy level may be labeled with the K values of the symmetric rotor

levels which it "connects" as $J_{K_{-1},K_{+1}}$; K_{-1} being the prolate value and K_{+1} the oblate value.

The following relations exist between τ and K_{-1} , K_{+1} ;

$$\tau = K_{-1} - K_{+1}$$
,
 $K_{\pm 1} = \frac{J \pm \tau}{2} + \{ \begin{smallmatrix} 0 \\ 1/2 \} \}$ (to make $K_{\pm 1}$ integral).
(2-27)

The frequency of a transition in the microwave spectrum from an initial level of energy W_1 to one with energy W_2 is given by the Bohr condition $v = \frac{W_2 - W_1}{h}$. (2-28)

A transition is allowed only if it may have a non-zero intensity. This restricts ΔJ to values of -1, 0, 1 (called P, Q, R branch transitions) and ΔK_{-1} , ΔK_{+1} to values listed below depending on the principal axis orientation of the permanent electric dipole moment μ .

Component of µ along	ΔK_{-1}	ΔK_{+1}
a axis (a type transitions)	even	odđ
b axis (b type transitions)	odd	odd
c axis (c type transitions)	odd	even

The dipole moment for an asymmetric top molecule does not necessarily lie along one principal axis (as it must for a symmetric top), but may have components along any or all of the axes. Thus the a, b, and c type transitions are not in general mutually exclusive. Symmetry within a molecule, however, may limit the orientation of μ and allow components along only one or two of the principal axes.

The symmetry of the rigid asymmetric rotor wave functions has been examined by King, Hainer, and Cross (18). The Hamiltonian belongs to the Four-group, V(a,b,c), which has the operations E, C_2 ,

 C_2 , C_2 . The character table for V(a,b,c) is shown below, with the final column listing the symmetry class for a rotational level of $J_{K_{-1}K_{+1}}$. It will be noted that the symmetry depends only on the relative odd and even nature of the K's.

Character Table and Symmetry Classification for the Group V(a,b,c)

Species representation	E E	perati C ₂	on C ₂	C ₂	Symmetry of $K_{-1}K_{+1}$
А	+1	+1	+1	+1	e e
$B_{\mathbf{a}}$	+1	+1	-1	-1	e o
B _b	+1	-1	+1	-1	0 0
Вс	+1	-1	-1	+1	o e
					e = even, o = odd

2.3 Perturbations to the Rigid Rotor

A) Stark Effect

The rigid rotor energy levels are (2J + 1)-fold degenerate in the spatial quantum number M in the absence of a unique space-fixed axis. The application of an electric field establishes a unique (field) direction, producing a molecular Stark effect through the interaction between the field and the molecular electric dipole moment.

The Stark effect eigenvalues are obtained by adding a potential energy term $-\overline{\mu} \cdot \overline{\xi} \cdot (\overline{\mu})$ is the molecular electric dipole moment vector and $\overline{\xi}$ the electric field vector) to the rigid rotor Hamiltonian. $\overline{\mu}$ is then transformed from its molecule-fixed axis system to the space-fixed axis system by the direction cosine transformation,

$$\mu_F = \sum_g \Phi_{Fg} \mu_g \ , \label{eq:fixed} \qquad \qquad (2-29)$$

$$F = X, Y, Z, \text{ the space fixed axes,}$$

$$g = x, y, z, \text{ the molecule fixed axes.}$$

The solutions for the non-degenerate asymmetric rotor take the form (19)

$$W_s = \epsilon^2 \sum_{\alpha} (A_{\alpha} + B_{\alpha}M^2)\mu_{\alpha}^2, \quad \alpha = a, b, c,$$
 (2-30)

where A_{α} , B_{α} are calculated from second order perturbation terms of the type

$$\frac{\left[\langle J,\tau,M|\widetilde{T}\widetilde{X}\Phi_{F\alpha}XT|J',\tau',M'\rangle\right]^{2}}{W_{J,\tau}-W_{J',\tau'}},$$
(2-31)

where $\Phi_{F\alpha}$ is a direction cosine matrix. The solutions are functions of the quantum numbers and molecular parameters.

The three major applications of the Stark effect are: (1) to modulate the absorption signals, thereby greatly increasing instrumental sensitivity; (2) to aid in assigning quantum numbers to an observed transition by the characteristic pattern of the Stark effect; and (3) to determine the molecular dipole moment components from the change in the perturbation energy with a change in the electric field strength.

B). Nuclear Quadrupole Coupling

The measurement of nuclear quadrupole hyperfine effects in rotational spectroscopy is of interest because the quadrupole coupling constants obtained provide information about the electronic configuration (bonding) in the molecule.

Quadrupole effects arise from the coupling of the nuclear spin angular momentum of an atom possessing a nuclear quadrupole moment with the rotational angular momentum. This coupling is the electrostatic interaction between the non-spherical (quadrupolar) nuclear charge and the entire extra-nuclear charge distribution. The interaction energy is different for each orientation of the nucleus with respect to the entire molecule.

The method of calculating the perturbation energies produced by the presence of one quadrupolar nucleus in an asymmetric rotor will be briefly outlined, utilizing the results of Casimir (20) and Bragg and Golden (21). The energy is a function of the nuclear quadrupole moment Q, the nuclear spin I, and the gradient of the electric field, $\overrightarrow{\nabla} \in$, at the quadrupolar nucleus. The field gradient is equal to $\overrightarrow{\nabla} \overrightarrow{\nabla} \vee V$, where V is the electrostatic potential at the nucleus due to the entire extra-nuclear charge distribution.

The perturbation Hamiltonian for the interacting nuclear quadrupole is

$$H_{Q} = eQ \left\langle \frac{\partial^{2}V}{\partial Z^{2}} \right\rangle_{AV}. \quad \left[\frac{3(\overline{J}^{2} \cdot \overline{I}^{2})^{2} + 3/2(\overline{J}^{2} \cdot \overline{I}^{2}) - J^{2}I^{2}}{2J(2J-1) \ I \ (2I-1)} \right]$$
 (2-32)

where e is the electronic charge,

J is the total angular momentum for the rigid rotor molecule, and $\frac{\partial^2 V}{\partial z^2}$ Av. is the average field gradient at the nucleus in the Z direction, the direction of J.

The numerator of the term in square brackets has eigenvalues derived by Casimir to be 3/4 C(C + 1) - I(I + 1)J(J + 1), where C = F (F + 1) - I(I + 1) - J(J + 1), and (2-33) $F = J + I, J + I - 1, \cdots, |J - I|.$

The total angular momentum quantum number F is a constant of the motion and hence a good quantum number. The levels are normally labeled with F, J, τ , where J and τ are the quantum numbers of the level in the limit of zero coupling. Therefore the effect of a quadrupole coupling is to split each pure rotational level in 2I + 1 (or 2J + 1, whichever is smaller) levels.

Bragg and Golden evaluated $\frac{\partial^2 V}{\partial Z^2}$ Av. using first order perturbation to be

$$\frac{2}{h(2J+3)(J+1)} \left[q_{aa} \frac{\partial^{1} r}{\partial A^{2}} + q_{bb} \frac{\partial^{1} r}{\partial B^{2}} + q_{cc} \frac{\partial^{1} r}{\partial C^{2}} \right], (2-34)$$

where q_{aa} etc. are the field gradients $\frac{\partial^2 V}{\partial a^2}$ in the direction of the principal axes,

and $\frac{\partial W_r}{\partial A}$ etc. have been defined in (2-26).

By defining several new terms the quadrupole interaction energy may be more simply expressed. The quadrupole coupling constants are

$$\chi_{aa}$$
 = eQ q_{aa},
 χ_{bb} = eQ q_{bb}, and (2-35)
 χ_{cc} = eQ q_{cc},

and within the validity of the Laplace equation ($\overrightarrow{\nabla}$ $\overrightarrow{\nabla}$ V = 0), Υ_{aa} + Υ_{bb} + Υ_{cc} = 0. Thus there are only 2 independent coupling constants, which may be taken to be Υ_{aa} and (Υ_{bb} - Υ_{cc}). Casimir's function Y(F,I,J) is

$$Y(F,I,J) = \frac{3/4 C(C+1) - I(I+1)J(J+1)}{2I(2I-1)(2J-1)(2J+3)}$$
(2-36)

and has been tabulated for values of I and J.

The quadrupole perturbation energy, W_{Ω} , may now be written as

$$W_{Q} = \frac{2}{J(J+1)} Y(F,I,J) \left[\frac{\partial W_{r}}{\partial A} \chi_{aa} + \frac{\partial W_{r}}{\partial B} \chi_{bb} + \frac{\partial W_{r}}{\partial C} \chi_{cc} \right], (2-37)$$

and further simplified to

$$W_0 = \alpha_{\sigma} \chi_{aa} + \beta_{\sigma} (\chi_{bb} - \chi_{cc}) , \qquad (2-38)$$

by defining

$$\alpha_{\mathbf{q}} = \frac{Y(\mathbf{F}, \mathbf{I}, \mathbf{J})}{J(J+1)} \left[2 \frac{\partial W_{\mathbf{r}}}{\partial A} - \frac{\partial W_{\mathbf{r}}}{\partial B} - \frac{\partial W_{\mathbf{r}}}{\partial C} \right], \text{ and}$$

$$\beta_{\mathbf{q}} = \frac{Y(\mathbf{F}, \mathbf{I}, \mathbf{J})}{2J(J+1)} \left[\frac{\partial W_{\mathbf{r}}}{\partial B} - \frac{\partial W_{\mathbf{r}}}{\partial C} \right].$$

Values for the coupling constants may be obtained from an analysis of the hyperfine splittings observed in the rotational spectrum.

2.4 Determining a Molecular Structure

In section 2.2 moments of inertia were calculated from the structure of a molecule. The inverse procedure of determining an unambiguous structure from the observed moments of inertia is not so simple.

Three rotational constants are the maximum available data, but in general there are 3n - 6 coordinates to be determined, although this may be reduced by symmetry assumptions. Isotopic substitution, therefore, is used to provide more information: an isotopic atom is substituted for an atom in the original molecule and another set of rotational constants is obtained from the spectrum. To gain information in this way it is necessary to assume that the structure is unaffected by the substitution. This is precisely valid only for the equilibrium structure, since the rotational measurements are time-

averaged over the ever-present vibrational motions, and these in turn are altered by isotopic substitution. Therefore some of the high precision of microwave measurements is sacrificed to vibrational effects in order to gain structural information.

In 1952 Kraitchman (11) systematically described the details of determining a molecular structure from isotopic substitution data, and the following discussion is based on his work. It is necessary to neglect vibrational effects at this point, but they will be considered later.

For a molecule in its principal axis system

$$\sum_{i} m_{i}a_{i} = 0 ,$$

$$\sum_{i} m_{i}b_{i} = 0 ,$$

$$\sum_{i} m_{i}c_{i} = 0 ,$$

$$P_{ab} = \sum_{i} m_{i}a_{i}b_{i} = 0 ,$$

$$P_{ac} = 0 ,$$

$$P_{bc} = 0 ,$$

$$P_{bc} = \sum_{i} m_{i}a_{i}^{2} ,$$

$$P_{bb} = \sum_{i} m_{i}b_{i}^{2} ,$$

$$P_{cc} = \sum_{i} m_{i}c_{i}^{2} ,$$
 and
$$M = \sum_{i} m_{i} ,$$
 the molecular weight.

If the mass of the s^{th} atom is increased by an amount Δm , the new principal axis system will occur with its center of mass shifted by

 $\frac{\Delta ma_s}{M+\Delta m}$, $\frac{\Delta mb_s}{M+\Delta m}$, $\frac{\Delta mc_s}{M+\Delta m}$ from the parent center of mass and generally rotated with respect to the parent axes.

The elements of P for the substituted molecule, calculated in the parent principal axis system, will be of the form

$$P'_{aa} = \sum_{i} m'_{i} a_{i}^{2} - \frac{\left(\sum_{i} m'_{i} a_{i}\right)^{2}}{\sum_{i} m'_{i}}, \text{ etc.,}$$

$$P'_{ab} = \sum_{i} m'_{i} a_{i} b_{i} - \frac{\left(\sum_{i} m'_{i} a_{i}\right)\left(\sum_{i} m'_{i} b_{i}\right)}{\sum_{i} m'_{i}}.$$
(2-41)

Since the only difference between these summations and those for the parent is that $m_S^1 = m_S^2 + \Delta m$, the equations reduce to

$$P_{aa}^{\prime} = P_{aa} + \Delta ma_{s}^{2} - \frac{(\Delta m)^{2} a_{s}^{2}}{M + \Delta m}$$

$$= P_{aa} + \mu a_{s}^{2} , \qquad \text{etc.},$$

$$P_{ab}^{\prime} = \Delta ma_{s}b_{s} - \frac{(\Delta m)^{2} a_{s}b_{s}}{M + \Delta m}$$

$$= \mu a_{s}b_{s} , \qquad \text{etc.},$$

$$where \mu = \frac{M\Delta m}{M + \Delta m} .$$

The experimental second moments $(P_{aa}^{"})$ for the substituted molecule are the roots, $P_{aa}^{"}$, of the determinant

$$P_{aa} + \mu a_{s}^{2} - P''$$
 $\mu a_{s}^{b} b_{s}$
 $\mu a_{s}^{c} c_{s}$
 $\mu a_{s}^{c} c_{s}$

When the determinant is expanded and the coefficients of powers of P" are set equal to the respective coefficients for the polynomial

$$P''^{3} - P''^{2}(P'_{aa} + P'_{bb} + P'_{cc}) + P''(P'_{aa}P'_{bb} + P'_{aa}P'_{ca} + P'_{bb}P'_{cc}) - P'_{aa}P'_{bb}P'_{ca} = 0$$
 (2-44)

three equations in the three coordinates result. These may be solved to give equations for the coordinates as

$$|a_{s}| = \{\mu^{-1} \left[\frac{(P_{aa}^{"} - P_{aa})(P_{bb}^{"} - P_{aa})(P_{cc}^{"} - P_{aa})}{(P_{bb} - P_{aa})(P_{cc} - P_{aa})} \right] \}^{1/2}$$

$$= \{\mu^{-1} (P_{aa}^{"} - P_{aa})(1 + \frac{P_{bb}^{"} - P_{bb}}{P_{bb}^{"} - P_{aa}})(1 + \frac{P_{cc}^{"} - P_{cc}}{P_{cc}^{"} - P_{aa}}) \}^{1/2}.$$
(2-45)

Equations for $|b_s|$ and $|c_s|$ may be obtained by cyclic permutations of a, b, c.

The signs of the coordinates must be determined from other information, often chemical information such as the bonding skeleton and plausible values for bond lengths and bond angles. Furthermore, for complete substitution at all non-equivalent sites the final coordinates with their signs must satisfy the center-of-mass conditions and give reasonable values of I_a , I_b , and I_c .

2.5 The Coupling of Vibration and Rotation

Some of the problems of vibrational origin which are encountered in determining a molecular structure may be demonstrated by considering the perturbation of vibration-rotation coupling in some detail.

The following discussion will also form the basis for the discussion of the vibration-rotation coupling observed for 1,3,2-dioxaborolane.

The effect of molecular vibrations on the rotational constants is rather straightforward in principle but highly complex in practice. The evaluation of the effects of vibration-rotation coupling is usually stymied by the lack of information concerning the normal coordinates and the vibrational force constants. There are two vibrational effects on the rotational energy levels, and thereby on the rotational constants, which must be considered.

The first effect arises from Coriolis coupling. This coupling is due to the fact that the vibrations are observed in a rotating coordinate system. As a result an angular momentum term associated with both the vibrations and the rotation must be included in the total Hamiltonian. Generally the large contributions of angular momentum arising from degenerate or near-degenerate vibrations are absorbed into the vibrational Hamiltonian. The remaining contributions are included in the rotational Hamiltonian, since a perturbation calculation for them yields terms which are quadratic in angular momentum, and hence are indistinguishable from the terms arising from ordinary rigid rotation. The result of this inclusion of Coriolis terms is to alter the rotational constants, making them no longer strictly proportional to the inverse of the moments of inertia at equilibrium.

The second effect arises from the dependence of the values of the principal moments of inertia on the actual vibrational motions of the atoms. This dependence may be elucidated by considering the vibrational motion of each atom in the molecule.

To start, the Cartesian coordinants measuring the instantaneous displacement of each atom from equilibrium may be written as a linear combination of the 3N-6 normal coordinants Q_K ,

$$\delta \alpha_{i} = m_{i}^{1/2} \sum_{K=1}^{3N-6} 1_{iK}^{\alpha} Q_{K},$$
 (2-46)

where
$$\delta \alpha_i = \alpha_i^e - \alpha_i^{inst.}$$
.

The six Eckart conditions (23),
$$\sum_{i} m_{i} \delta \alpha_{i} = 0$$
 etc., (2-47)

$$\sum_{i} m_{i} (\alpha_{i}^{e} \delta \beta_{i} + \beta_{i}^{e} \delta \alpha_{i}) = 0$$
 etc.

complete the transformation. These conditions assure maximum uncoupling of the vibration and rotation, and establish a linear dependence between the 3N-6 normal coordinates and 3N 6 α_i .

The instantaneous moments of inertia may then be expressed in terms of the equilibrium and displacement of coordinates as

$$I_{\alpha\alpha}^{inst.} = \sum_{i} m_{i} [(\beta_{i}^{inst})^{2} + (\gamma_{i}^{inst})^{2}]$$

$$= \sum_{i} m_{i} [\beta_{i}^{e^{2}} + \gamma_{i}^{e^{2}}] + 2 \sum_{i} m_{i} [\beta_{i}^{e} \leq \beta_{i} + \gamma_{i}^{e} \leq \gamma_{i}]$$

$$+ \sum_{i} m_{i} [(\beta_{i}^{e})^{2} + (\delta_{i}^{e})^{2}], \qquad (2-48)$$

and similarly for the products of inertia,

$$I_{\alpha\beta}^{inst} = -\sum_{i} m_{i} \alpha_{i}^{e} \beta_{i}^{e} - \sum_{i} [m_{i} \alpha_{i}^{e} \delta \beta_{i} + \beta_{i}^{e} \delta \alpha_{i}]$$

$$-\sum_{i} m_{i} (\delta \alpha_{i}) (\delta \beta_{i}).$$
(2-49)

The first term in (2-49) is zero by the definition of the equilibrium principal axis system, and the second term is zero by the Eckart condition.

These expansions demonstrate that the vibrations contribute both diagonal and off-diagonal terms to the instantaneous moment of inertia tensor. In order to express the effective moments of inertia, it is necessary to average the instantaneous values over the vibrational motions. The correct averaging is of the rotational constants over the vibrational motions, since this is what actually occurs in an experimental measurement. Therefore, it is necessary to invert the instantaneous moment of inertia tensor before taking the vibrational average.

The elements of the inverse instantaneous tensor $(I^{inst})^{-1}_{\alpha\beta}$ may be expressed as power series in the normal coordinates as

$$(\text{I}^{\text{inst}})_{\alpha\beta}^{-1} = \frac{\delta \alpha\beta}{\text{I}_{\alpha\beta}^{e}} - \sum_{K} a_{K}^{\alpha\beta} Q_{K} - \sum_{K} \sum_{M} (A_{KM}^{\alpha\beta} - \sum_{Y} a_{K}^{\alpha\gamma} a_{M}^{\beta\gamma}/\text{I}_{Y}^{e})Q_{K}Q_{M} - \cdots$$
where
$$a_{K}^{\alpha\beta} = (\frac{\partial \text{I}_{\alpha\beta}^{\text{inst}}}{\partial Q_{V}}) \quad \text{and} \quad A_{KM}^{\alpha\beta} = (\frac{\partial \text{I}_{\alpha\beta}^{\text{inst}}}{\partial Q_{V} \partial Q_{M}}). \quad (2-50)$$

After averaging over the vibrational motions, the resulting expressions are re-inverted to yield effective moment of inertia terms.

$$[\langle (I^{inst})_{\alpha\beta}^{-1} \rangle]^{-1} \stackrel{:}{=} I_{\alpha\beta}^{v} = I_{\alpha\beta}^{e} \delta_{\alpha\beta} + \sum_{K} a_{K}^{\alpha\beta} \triangleleft_{K} \rangle + \sum_{K} (A_{KK}^{\alpha\beta} - a_{K}^{\alpha\gamma} a_{K}^{\beta\gamma} / I_{\gamma})$$

$$< Q_{K}^{2} > + \cdots . \quad (2-51)$$

The cross terms of $<Q_K^Q_M>$ contribute to higher order than that indicated for the expansion (2-51). Next the vibrational averages of the Coriolis terms must be added. Herschbach and Laurie (24) have shown these to be

$$-4 \sum_{K} \sum_{M}^{\prime} \left[\underset{KM}{\overset{\alpha}{\downarrow}} \underset{KM}{\overset{\beta}{\downarrow}} \frac{\lambda_{K}}{(\lambda_{K} - \lambda_{M})} \right] < Q_{K}^{2} > , \qquad (2-52)$$

where $\mathcal{L}_{KM}^{\alpha}$, \mathcal{L}_{KM}^{β} are the Coriolis coupling constants,

and $\boldsymbol{\lambda}_{K},~\boldsymbol{\lambda}_{M}$ are the vibrational eigenvalues.

The final result is that the effective moments of inertia may be written as an expansion in average values of powers of the normal coordinates.

$$I_{\alpha\alpha}^{eff} = I_{\alpha}^{e} + \sum_{K}^{K} C_{1}^{K} < Q_{K}^{2} > + \sum_{K}^{K} C_{2}^{2} < Q_{K}^{2} > + \cdots$$
 (2-53)

The coefficients C_1^K etc. may be evaluated if sufficient data are available. When this is not possible, they may be treated as empirical parameters.

Two further simplifications are possible. The first is the single mode approximation. In this scheme contributions to I_{eff} from all vibrational modes except the one being considered (K = 1) are assumed to be separable. It is assumed that the interactions of the other modes may be included in the coefficients C_1^1 , C_2^1 etc. As a result $I_{\alpha\beta}^{eff}$ becomes

$$I_{\alpha\beta}^{eff} = I_{\alpha\beta}^{e} \delta_{\alpha\beta} + C_{1}^{1'} < Q_{1} > + C_{2}^{1'} < Q_{1}^{2} > + \cdots$$
 (2-54)

This approximation is generally used when there is one mode which dominates the vibration-rotation interaction, and little or no data is available for the other modes.

The second simplification results in the familiar vibrationrotation coupling equations

$$B_{v} = B_{e} - \sum_{K} \alpha_{K}(v_{K} + 1/2 d_{K}),$$
 (2-55)

and the equivalent equation $I_v = I_e + \sum_K \epsilon_K (v_K + 1/2 d_K)$. These

equations may be obtained from (2-53) by noting that the quantum dependence of $<Q_K^2>$ for an harmonic oscillator is $(v_K+1/2\ d_K)$. Furthermore, the leading terms in a perturbation treatment of $<Q_K>$ have this dependence also. Consequently the coefficients of all the terms may be combined to form the α_K of ϵ_K . Most of the values of α_K which have been determined are small positive numbers.

The preceding discussion indicates that in cases where the vibration-rotation coupling is small, the rotational spectrum can retain the features of a rigid rotor. The effective rotational constants depend on the vibrational state, and there may be several rotational spectra, each due to a different vibrational state. The degree to which each spectrum fits a rigid rotor pattern is a measure of the relative perturbation caused by the coupling of vibrations.

To examine the effect of vibrations on molecular structures determined from isotopic data, it is necessary to ascertain which quantities change in value with the substitution.

The most obvious changes are in the vibrational frequencies of normal modes which contain large motions of the substituted atom. For diatomic molecules \in_K is proportional to $(\nu_K)^{-1}$, so the decrease in the vibrational frequency which occurs upon substitution of a heavier isotope causes an increase in \in_K . This means that the effective moment of inertia for the substituted molecule is even larger than would be predicted by the simple mass increase.

A second, less obvious, change upon isotopic substitution is in the effective bond lengths. These in general decrease with the substitution of a heavier atom. This is due to the fact that the energy

levels are now lower in the vibrational potential well, so the amplitude of vibration is decreased, and the average value of the bond length is smaller. This effective bond shortening has the greatest primary effect when deuterium is substituted for hydrogen, but also may be observed as a secondary effect on a bond A-B when C is the substituted atom.

A third quantity which changes on isotopic substitution is the inertial defect. For the equilibrium structure of a planar molecule $I_c^e - I_a^e - I_b^e$ must be zero. A vibrating planar molecule has an inertial defect Δ_v defined as $\Delta_v = I_c^v - I_a^v - I_b^v$. (2-56) Actually, the inertial defect is a single term containing the effects arising from vibration-rotation coupling for the totality of the vibrational motions. It is a convenient parameter because it has been determined for many planar and near-planar molecules, and good methods for calculating its value have been devised, most notably in the work of Oka and Morino (25), and Laurie and Herschbach (26).

The fact that the inertial defect is a single term for all the vibration-rotation coupling makes it convenient both for numerical calculations and qualitative explanations. In addition the concept of a quasi-inertial defect is a convenient one in examining the structure of molecules which are near-planar, or which are composed of a large planar portion with a small out-of-plane component; for example, a molecule like acetaldehyde in which only two of the methyl hydrogens do not lie in the symmetry plane. In such a case the non-zero z coordinates could be obtained from the equation

$$\mu_{H} z_{H}^{2} = I_{A}^{0} + I_{B}^{0} - I_{C}^{0} + \Delta_{0}$$
(2-57)

if an estimate of Δ_0 is available; or with substitution of deuterium for the hydrogen nuclei from the equation

The following statements are generally accepted as guides to the problems and errors which are encountered in the determination of the parameters of a molecular structure (12).

- 1) Parameters which are obtained by using experimental moments of inertia in equations which are satisfied only by equilibrium values, generally deviate from equilibrium values. A structure calculated in this fashion is called an r_0 structure.
- 2) Coordinates which are obtained by using only differences in the moments of inertia of two isotopic species also differ from the equilibrium values, but are generally closer to the equilibrium values than are the r_0 parameters. Furthermore, the coordinates are generally smaller than the equilibrium values when the substitution introduces a heavier isotope. A structure calculated solely from the differences in moments of inertia of pairs of isotopic species is called the $r_{\rm g}$ structure.
- 3) A large uncertainty is expected in the location of a light atom, particularly an H atom, if its r_0 coordinates are determined.
- 4) A large uncertainty is expected in the coordinates of an atom located near an inertial plane. In general the calculated distance from the plane will be less than the equilibrium distance. Even if this distance was determined from equilibrium values of the moments of inertia, its uncertainty may be large, being proportional to the

uncertainty in I^e divided by the distance from the plane. A classic example of this type of behavior is the linear molecule N_2O . Substitution of the heavier isotope ^{15}N for ^{14}N in $^{15}N^{14}N^{16}O$ produces a decrease in the moment of inertia. As a result an imaginary value for the ^{14}N coordinate is obtained. (27).

The general validity of these statements may be demonstrated by some simple considerations based on the simplified results of vibration-rotation coupling which were presented above.

The greatest uncertainties in the structural parameters are due to the vibrational motions which shift the effective moments of inertia from their equilibrium values. For ro structures, all the vibration-rotation coupling is absorbed into the coordinates; necessarily moving the atoms to compensate for the differences ($I^{o}-I^{e}$). This is a result of presuming that the values of IO are compatible with the equations in the equilibrium coordinates. Less uncertainty is present in r_s structure, since in this case the atoms are moved to compensate only the differences (\sum_{K} (ϵ_{K}^{\prime} - ϵ_{K})). The non-equality of r_{s} and equilibrium coordinates which has been observed indicates that $(\sum_{K} (\epsilon_{K}' - \epsilon_{K}))$ is not necessarily small enough to be consistently neglected. If a light atom must be moved to compensate the difference $I^0 - I^e$, the error in its coordinate will obviously be greater than if a heavy atom had been moved. On the other hand, with the substitution technique the error in the coordinates depends only on the difference in mass between the isotopes, so a light atom may be located with the same precision as a heavy atom.

III. DESCRIPTION OF THE MICROWAVE SPECTROMETER

3.1 Introduction

A conventional 100 kc/sec. Stark-modulated microwave spectrometer was used in this work. It consists of the following elements: a source of microwave radiation (klystron oscillator), a waveguide absorption cell, a square-wave generator for Stark modulation, a detection system, and a frequency measuring unit. Figure 1 is a block diagram of the spectrometer.

3.2 Klystron oscillators

At Michigan State University the sources of microwave power are reflex type klystron oscillators. In these devices a stream of electrons is obtained from a heated cathode. They are drawn toward an anode which is maintained at a positive bias, giving the electrons a high velocity. Some of the electron beam passes through a hole in the anode and is focussed to a gap which has been made part of a resonant circuit. An external radio-frequency field established in this circuit "bunches" the moving electrons by slowing or accelerating them depending on which part of the field cycle they encounter as they pass through the cavity. This series of electron packets then is reflected back into the resonant cavity by a negatively charged reflector. As they return through the cavity, the electrons induce a large r-f field and lose energy in the process. If the radiant energy emitted by the returning electrons is in the correct phase the

37

klystron resonates, producing an extremely monochromatic milliwatt microwave output.

Tuning the klystron is accomplished by varying the size of the cavity, thereby changing its resonant frequency. The tuning range is normally about 15-20% of the central design frequency. Changing the reflector voltage continuously between the values necessary to maintain oscillation provides fine tuning and normally has a range of 30-40 Mc/sec. The klystrons used in this work are listed in Table I with their frequency ranges. The frequency meter and crystal detector used for each frequency region is also listed.

The klystron is powered by an F.X.R. type Z815B power supply designed to provide beam voltages from 200-3600 volts, reflector voltages from 0 to -1000 volts, and grid voltages from 0 to -300 volts, all highly stabilized. An auxiliary supply provides a stable D.C. heating current for the filament.

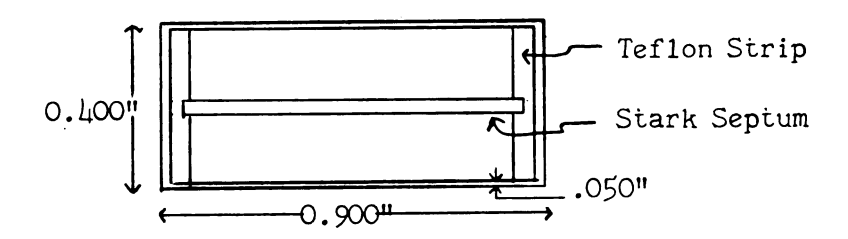
In order to use an oscilloscope to observe transitions, the klystron and oscilloscope must sweep over a short frequency range simultaneously. The simultaneous sweeping is accomplished by coupling the output of the X-axis sweep voltage from the oscilloscope to the reflector of the klystron through a D.C. isolation network. The klystron frequency then varies uniformly as the beam sweeps across the face of the oscilloscope. Thus the X-axis of the oscilloscope is a linear display of the klystron frequency. A sweep width of 1-10 Mc is normally used.

Table I. Klystrons, frequency meters, and crystal detectors now in use at Michigan State University.

Frequency (kMc/sec.)	K lys tron	Frequency Meter	Crystal Detector (Microwave Associates)	
8.2 to 12.6	Varian X-13	Narda 810	1N23	
12.4 to 18.0	Varian X-12	Narda 809	1N23 1N78	
18.0 to 22.5 22.5 to 26.0	EMI/US R9622 EMI/US R9602	DeMornay-Bonardi DBE-715-2	1N26 1N78	
26.0 to 30.0 27.9 to 32.3 32.0 to 37.5	Ratheon QK289 EMI/US R9518 EMI/US R9546	DeMornay-Bonardi DBD-715-2	1N26	

3.3 Waveguide Absorption Cell

The waveguide absorption cell is a ten foot section of rectangular brass X-band waveguide with cross section and dimensions as shown below. The inner surface is silver-lined for increased conductivity. Teflon strips with a 0.010 inch deep groove running their length are laid along the shorter walls to support and insulate the Stark septum, a coin-silver strip which runs the length of the cell. An electrical contact to the septum passes through a hole in the teflon and is sealed with an N-type connector and an O-ring seal. The entire cell is sealed at both ends with mica windows and O-ring seals and is kept at high vacuum. An attached vacuum line serves as a sample introduction and recovery system.



Teflon tape: 0.062" x 0.400" with 0.032" groove 0.010" deep. Coin silver septum: 0.032" x 0.796".

Figure 2. Stark waveguide cross section.

3.4 Square Wave Stark Modulation

Modulation of the absorption signal is provided by applying a 100 kc/sec square wave to the Stark septum. A second signal from the square wave generator is used as the reference signal for a phase-sensitive detector. If the klystron is at an absorption frequency,

the square wave produces a Stark effect which shifts the absorption, in essence turning the absorption at the given frequency on and off 100,000 times per second. As a result the microwave absorption signal is modulated at 100 kc/sec and may thus be detected by a phase-sensitive detector (or lock-in amplifier). A useful Stark effect requires rather high fields and consequently the amplitude of the square-wave must be variable up to at least 1000 volts.

3.5 Detection System

Two types of microwave power detectors are commonly used, silicon rectifiers and bolometers. The bolometer is a temperature sensitive impedance element. A constant current passed through it gives a voltage change as the resistance changes with incident microwave power. The silicon rectifier type of detector used at Michigan State University is a diode circuit element. It consists of a thin sheet of silicon in which a contact wire is imbedded. An A.C. signal is partially rectified to give a D.C. output voltage roughly proportional to the input A.C. power. The crystal is held in a mount which is tunable to provide maximum sensitivity.

The output of the crystal is sent to the inductance-capacitance circuit shown in Figure 3. The D.C. component passes through the parallel circuit (A) to a milliammeter to indicate the power level. The 100 kc/sec component is applied to the control grid of the first preamplifier tube.

The output from the preamplifier is applied to the signal input of a phase sensitive detector; a signal from the square wave generator

is applied to the reference input. If the signal from the preamplifier has the same frequency and phase as the reference, the output voltage of the phase-sensitive detector will be increased; if the frequency or the phase is different, the output will be suppressed.

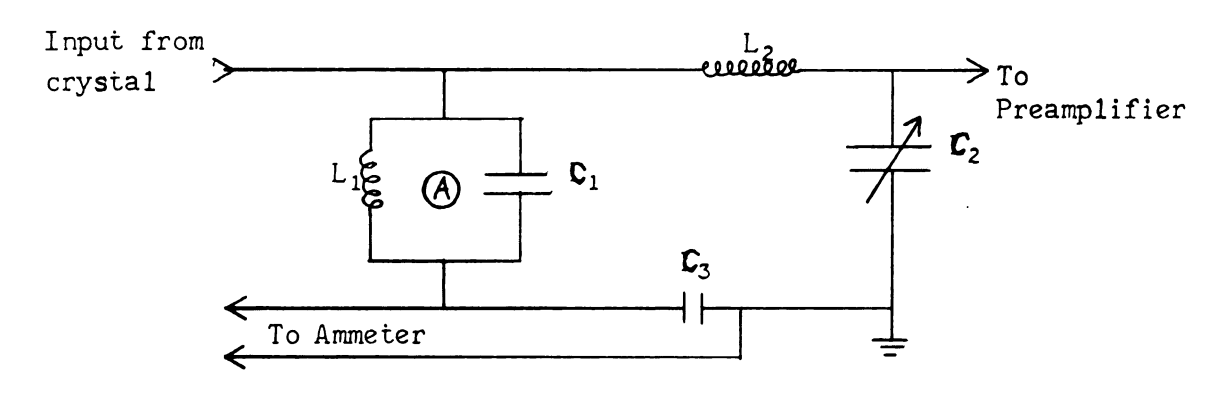


Figure 3. Detection preamplifier input circuit.

3.6 Frequency Measurement

Rough frequency measurements, as in initially locating a transition, are made with one of a series of resonant cavity frequency meters whose calibrations are supplied by the manufacturers. The klystron oscillator is driven either manually or with a small wormdrive motor. When an absorption peak is noted on the oscilloscope, the frequency meter is tuned until the power trace on the oscilloscope shows an 'absorption' resulting from loss of power to the meter at its resonant frequency. The scale reading of the frequency meter is then converted to the microwave frequency with a precision of 0.03% at best.

Precise frequency measurements are made by determining with a Collins 51J-4 radio receiver the difference between the microwave frequency and a generated standard frequency.

The corner-stone of the standard frequency generator is a Manson Model RD140 crystal-controlled 1 Mc/sec oscillator. The oscillator frequency is maintained by adjusting it until its 10th harmonic and the 10 Mc/sec carrier wave of National Bureau of Standards radio station WWV have a beat frequency of less than 1/2 cycle/second. Overall stability of at least one part in 10⁷ is obtained.

The 1 Mc/sec signal is input to a Gertsch AM-1A VHF interpolator composed of three units. The first is a frequency multiplier (VHF) with a selective stepped output of 19-38 Mc/sec. The second is a 1-2 Mc/sec low frequency oscillator (LFO) which may be adjusted to fixed known frequency by tuning until a stable Lissajous figure is obtained against the 1 Mc/sec oscillator signal. The sum of the multiplier and LFO signals is used to control the frequency of the third unit, a 20-40 Mc/sec oscillator which acts as a filter and amplifier.

The 1 Mc/sec oscillator signal and the 20-40 Mc/sec output of Am-1A are input to a Gertsch FM-4A microwave frequency multiplier. The FM-4A may be tuned to lock 10 Mc/sec above or below a harmonic of the 20-40 Mc/sec input. The output is an accurately produced signal in the range 500-1000 Mc/sec plus harmonics.

The standard frequency generated in the microwave region may be calculated from the equation

$$v_{standard} = n[m(v_{LFO} + v_{VHF}) \pm 10],$$
 $n,m = 1,2,3,\dots,$
 $v_{LFO} = 1 \rightarrow 2,$
 $v_{VHF} = 19,20,\dots,38.$

(3-1)

The klystron output and the standard frequency signals are multiplied and mixed in a tunable crystal detector. The beat frequencies from this mixture pass through a 500 Mc/sec low-pass filter to the Collins receiver which functions as a tunable, extremely narrow bandpass filter and amplifier. The carrier wave is removed and the output of the receiver is the noise from the beat signal. This signal may be applied to the Y axis of one trace of the dual-beam oscilloscope. As the saw-tooth voltage causes the klystron frequency to beat against the marker with the (radio) selected beat frequency, a 'pip' appears on the oscilloscope. Both positive and negative beats are possible. For example; if the klystron is swept from 20,980 Mc/sec to 21,020 Mc/sec by the saw-tooth voltage, with the marker set at 21,000 (the 30th harmonic of a 700 Mc/sec signal), the beat frequency will vary from 20 to 0 and then 0 to 20 Mc/sec. If the receiver is tuned to 12 Mc/sec a pip will appear on the oscilloscope when the klystron frequency is 20,988 and when it is 21,012 Mc/sec. In the more usual procedure either the positive or the negative beat is used, the klystron range is set so that it does not straddle the marker frequency, and only one beat is observed. For example, if the marker is at 30,000 Mc/sec, the klystron swept from 30,010 to 30,040, and the receiver set at 20 Mc/sec, one pip will be observed at 30,020 Mc/sec.

Since the marker and absorption signals have different amplification times, the average of two frequency measurements made with opposite sweep directions is used.

Frequency measurements are made using the oscilloscope display whenever it is possible to observe the transition on the oscilloscope trace. When this is not possible because either the transition

is too weak or it is desired to scan a wide region of the spectrum, measurements may be made on a recording. To accomplish this the D.C. output of the phase sensitive detector is input to a recording potentiometer while the klystron frequency is varied by changing the cavity size with the motor. Marker pips are made on the spectrum by noting the points ("whistle-through") at which the klystron frequency and the standard frequency differ by the frequency at which the radio receiver is set.

IV. MICROWAVE STUDIES ON 1,3,2-DIOXABOROLANE

4.1 Introduction

This chapter reports the microwave spectroscopic experiments performed on 1,3,2-dioxaborolane. It begins with a description of the chemical method of preparation for each of the samples which were studied. Next the transitions observed and the rigid rotor and quadrupole coupling constants deduced from the spectrum are presented.

Then a model for the molecular configuration is assumed; some of the effects anticipated from this model are described; and the experimental observations and conclusions supporting the assumed model are presented. Following this the most plausible structure for the compound is determined. Finally, the vibrational aspects are considered in some detail. A model for the low-frequency vibrational mode is assumed and the consistency of the many observed vibrational effects with this model is demonstrated. The implications on the form of the vibrational potential function are then discussed.

4.2 Preparation of Samples

Samples of 1,3,2-dioxaborolane (OCH_2CH_2OBH) were prepared by the addition reaction of diborane (B_2H_6) and ethylene glycol ($HOCH_2CH_2OH$) following the procedure of Rose and Shore (15) and with the aid of Dr. Shore and his students, Gerald McAchran and Gerald Brubaker.

Materials:

- Ethylene glycol was refluxed over sodium for 1 hour and vacuum distilled,
- 2. Diborane was vacuum distilled at -1200 to remove contaminants,
- 3. $N(CH_3)_3$ was purchased from Olin Matheson and used without further purification,
- 4. Ethyl ether was dried over LiAlH4 and vacuum distilled,
- 5. The following slush baths were used:
 - -120° Skelly solve F,
 - 780 Dry ice/isopropanol,
 - 63° Chloroform,
 - 45° Chlorobenzene,
 - 350 1,2-Dichloroethane.

<u>Procedure</u>: The preparation procedure may be summarized by the three reactions:

(A)
$$HOCH_2CH_2OH + 1/2 B_2H_6 \xrightarrow{Et_2O} OCH_2CH_2OBH + H_2^{\dagger}$$

(B)
$$OCH_2CH_2OBH + N(CH_3)_3 \longrightarrow OCH_2CH_2OBHN(CH_3)_3$$

(C)
$$OCH_2CH_2OBHN(CH_3)_3 + 1/2 B_2H_6 \stackrel{>}{\longleftarrow} OCH_2CH_2OBH + H_3BN(CH_3)_3$$

1,3,2-dioxaborolane is produced in step (A) but it is necessary to react it with $N(CH_3)_3$ to form a low vapor pressure adduct in step (B) to allow removal of the ether solvent. The free product is regenerated in step (C) by taking advantage of the greater Lewis acid strength of B_2H_6 in forming an adduct with the $N(CH_3)_3$.

In a 'dry box' 0.55 ml. (10 mmole) of ethylene glycol was transferred to a 100 ml. reaction flask containing a magnetic stirring bar and closed by a stopcock. The flask was cooled to -1960 and evacuated. Approximately 35 ml. of ether was distilled into the flask. The mixture was warmed until the ethylene glycol melted and was then cooled to -1960 while stirring vigorously to disperse the slightly soluble ethylene glycol. A previously measured 6.9 mmole amount of diborane was distilled into the reaction flask and the mixture was warmed to -780 with continuous stirring. A small amount of hydrogen was evolved and was pumped off after trapping any unreacted B_2H_6 at -1960. The trapped B_2H_6 was distilled back into the flask. When the rate of H_2 evolution became negligible, the flask was allowed to warm to -450 at which temperature the majority of the H_2 was evolved. The trapping and pumping was repeated. When H_2 evolution again became negligible the reaction was completed at room temperature.

To form the adduct, $QCH_2CH_2OBHN(CH_3)_3$, and remove unreacted B_2H_6 , 1.5 ml. (approximately 17 mmoles) of trimethylamine was distilled into the reaction flask and was allowed to react while stirring at -78°. The reaction was completed by stirring 2 hours at -45°. The ether was distilled from the reaction flask at -63°, and the last trace removed by pumping on the system at -45°.

The product was sublimed at room temperature into a 1 liter pear-shaped exchange flask equipped with a test-tube bottom to allow immersion in a dewar flask. Then 12.5 mmoles of B_2H_6 was distilled into the exchange flask, and the mixture was warmed to 50°. After two hours the contents of the exchange flask was passed very slowly

through a train of cold traps at -35°, -120°, and -196°. The 1,3,2-dioxaborolane was retained in the center trap. Unreacted B_2H_6 and the trimethylamine adducts were distilled back into the exchange flask. The exchange and fractional trapping was repeated 3 times. The 1,3,2-dioxaborolane in the -120° trap was quickly warmed to 40° and transferred to an evacuated, flame-dried, sample bulb. The bulb was stored at -78° or -196° until samples were needed.

A sample of 4,4,5,5-tetradeutero-1,3,2-dixoaborolane was prepared following the same procedure as for the parent species. The deuterated ethylene glycol was purchased from Merck, Sharp, and Dohme of Canada, as 98+ mole percent in methylene deuterium. It was vacuum distilled over sodium before use.

A sample of $(4)^{13}$ C - 1,3,2-dioxaborolane was prepared following the same procedure, starting with 13 C ethylene glycol. The glycol had been synthesized by the procedure summarized by the reactions:

1)
$$KC^*N + CH_3I \longrightarrow CH_3C^*N \xrightarrow{NaOH} CH_3C^*OONa$$

2)
$$CH_3C^*OONa + \varphi - CH_2C1 \longrightarrow CH_3C^*OC1$$

3)
$$CH_3C^*OC1 \xrightarrow{LAH} > CH_3C^*H_2OH$$

4)
$$CH_3C^*H_2OH \xrightarrow{A1_2O_3} > CH_2C^*H_2 \xrightarrow{Br_2} > BrCH_2C^*H_2Br$$

The starting material was 5.3 grams of KCN containing 19 mole% ¹³C. Sodium acetate was prepared from the KCN following the modified method of Cox, Turner, and Warne as reported in Murray and Williams, Organic Syntheses with Isotopes (28). The KCN was placed in a flask which had two male standard taper joints separated by a seal-off

constriction. Twelve ml. of water was added and the flask was attached to a vacuum line, frozen, and evacuated. Seven and one-half ml. of CH₃I was distilled into the flask, which was then sealed between the joints and shaken overnight. The flask was cracked open and the volatile contents vacuum distilled into 8 ml. of 20N NaOH. The hydrolysis of the methyl cyanide was completed by heating at 78° under partial vacuum for 4.5 hours. The resulting solution of NaOOC*CH₃ was rinsed into a 300 ml. flask with water, 30 ml. of 6N H₂SO₄ and 99.8 g. Ag₂SO₄ were added by mistake; 1.0 grams should have been added. Nitrogen was slowly bubbled through the solution and the mixture was distilled into a cooled beaker containing 0.9925N NaOH. When the distillation was completed, the distillate was titrated to pH 8.8 as measured on a glass electrode pH meter. The solution was then evaporated to dryness. The yield was 90% of the theoretical amount.

Acety1 chloride was prepared with 9% yield by distilling the fused NaOOC*CH3 with benzoyl chloride in a flame dried micro-apparatus.

Ethanol was prepared in 98.5% yield by reducing the acetyl chloride with lithium aluminum hydride following the method of Cox and Turner (29). The hydride was placed in a flask equipped with an addition funnel and stirring bar, and attached to the vacuum line through a reflux trap with a cold finger. Diethylene glycol diethyl ether was added slowly through the funnel, while stirring and cooling the flask. The system was warmed to room temperature and pumped on for 1 minute to complete the hydrogen out-gassing. The

acety1 chloride was vacuum distilled in at 0° and the system was frozen to -78° and re-evacuated. The reduction was completed by stirring 2 hours at 0°. The desired ethanol was released by alcoholysis with 2-phenoxy ethanol. This was accomplished by heating at 90° under reflux for 15 minutes and then at 100° for 2 hours. Finally the ethanol was distilled from the mixture.

Ethylene bromide was then prepared from $\mathrm{CH_3C}^*\mathrm{H_2OH}$ following the method of Popplewell and Wilkings (30). The ethanol was slowly distilled up a 17" column containing $\mathrm{Al_2O_3}$ (100-200 mesh) heated to about 380°. At the top of the column was placed a cold finger and then a bubble trap containing bromine and glass wool. The ethylene formed by dehydration of $\mathrm{CH_3C}^*\mathrm{H_2OH}$ added $\mathrm{Br_2}$, yielding ethylene bromide. The distillation took about 4 hours and was completed by sweeping the system with $\mathrm{N_2}$. The excess bromine was vacuum distilled from the less volatile product.

The final step of the synthesis was the hydrolysis of the $\operatorname{BrCH}_2\operatorname{C}^*\operatorname{H}_2\operatorname{Br}$ to ethylene glycol. This was accomplished by refluxing a mixture of ethylene bromide and 25% excess of 1 molar $\operatorname{Na}_2\operatorname{CO}_3$. The hydrolysis took about 12 hours and was continued 1 hour after the mixture became homogeneous. The products were passed through an ion exchange column to remove the sodium salts. Finally the water was removed from the glycol by pumping on the vacuum line for 2 days at O^0 . The total yield of $\operatorname{HOCH}_2\operatorname{C}^*\operatorname{H}_2\operatorname{OH}$ was about 2 ml.

The ¹³C enriched 1,3,2-dioxaborolane was prepared from the glycol by a different procedure from that used for the parent and deuterated compounds. This seemed to produce the product with less solvent contamination at the expense of a lower yield.

In a "dry box" 0.2 ml. of ethylene glycol and 5 ml. of decalin were placed in a reaction tube containing a magnetic stirring bar and equipped with a stopcock and a side arm with a \$ joint ending in a break-off seal. The tube was attached to the vacuum line, evacuated, and about 4 mmoles of B_2H_6 was distilled into it. Then the tube was sealed below the stopcock and allowed to warm to room temperature. The reaction was carried out by stirring the contents of the tube for 20 hours. The excess B_2H_6 and the product 1,3,2-dioxaborolane were vacuum distilled from the tube at room temperature into a sample tube. Finally, the diborane was distilled from the product at -120°.

A fourth isotopic species of 1,3,2-dioxaborolane, the ¹⁰B species was studied in its natural abundance (20%) in the parent sample.

4.3 Examination of the Rotational Spectra

Dr. R. H. Schwendeman began the analysis of the spectrum of 1,3,2-dioxaborolane by assuming some "reasonable" values for the molecular parameters (listed in Table II) by comparison with values obtained for other molecules. Then he calculated the moments of inertia and rotational constants for this structure, and used the rotational constants to predict a rotational spectrum. He examined the frequency region in the vicinity of several of the b-type low J transitions and assigned quantum numbers to the observed transition frequencies with the aid of the calculated Stark effects, quadrupole splittings, and intensities.

The initial analysis was complicated by the existence of a relatively intense second series of rotational transitions for the

Table II. Initial structural parameters assumed for 1,3,2-dioxa-borolane

В-Н	1.15 Å	∠ obo	1110 221	
B-0	1.38 Å	∠ BOC	109° 19'	
O-C	1.43 Å	∠ occ	105°	
C-C	1.54 Å	∠ HCH	1090 301	
C-H	1.10 Å	∠ HCC	1100 34'	
		∠ HCO	1100 341	

The B,O, and C atoms were assumed to be coplanar.

were confirmed by fitting the observed frequencies to a rigid rotor model. After the two series of transitions had been reduced to two rigid rotor sets, the responsibility for further studies of the spectra was assumed by the author of this thesis. A third series of transitions, similar to the first two, was later located and analyzed.

The work by both investigators was done with the absorption cell cooled to -78° with dry ice and with the sample at the lowest possible pressure consistent with workable intensity. All frequency measurements were made with oscilloscope display, although recordings were used to establish the presence of some of the small splittings caused by the 10 B nuclear quadrupole moment. An error of $^{\pm}$.02 Mc/sec. is estimated for most of the measurements.

The values of the rotational constants and quadrupole coupling constants were determined by a numerical least squares method. Starting with approximate values of A, B, and C, the values of α_q and β_q (the partial derivatives of the energy with respect to X_{aa} and $(X_{bb} - Y_{cc})$ as shown in Equation (2-38)) were calculated. Then X_{aa} and $(X_{bb} - X_{cc})$ were fit to the observed splittings between the quadrupole hyperfine components in each transition using equations of the form $\delta_V = \delta(\Delta\alpha_q) Y_{aa} + \delta(\Delta\beta_q) (Y_{bb} - Y_{cc})$. Here Δ is used (4-1) to indicate a difference between two energy levels and δ is used to indicate a difference between two frequencies, or between two energy-level differences. With these constants the quadupole coupling contribution to each component of a multiplet was calculated and was then subtracted from the observed frequency of the component. The average of these "hypothetical unsplit frequency" (H.U.F.) values was

taken as the rigid rotor frequency for the transition.

The rotational constants were then fit by using equations of the form

$$v_{o^{-}}v_{c} = \Delta \left(\frac{\partial W_{r}^{c}}{\partial A_{c}^{c}}\right) (A_{o} - A_{c}) + \Delta \left(\frac{\partial W_{r}^{c}}{\partial B_{c}^{c}}\right) (B_{o} - B_{c}) + \Delta \left(\frac{\partial W_{r}^{c}}{\partial C_{c}^{c}}\right) (C_{o} - C_{c}), \quad (4-2)$$

where the subscript o indicates observed values, and the subscript c indicates calculated trial values.

After an initial quadrupole fit was obtained, the caluclated hyperfine frequencies were corrected, where necessary, for small shifts (of the order of 0.05 Mc/sec.) due to the presence of unresolved hyperfine components.

The final values for A, B, C, $\chi_{\rm aa}$, ($\chi_{\rm bb}$ - $\chi_{\rm cc}$) were obtained by recycling the fitting procedure until a stability of better than 0.01 Mc/sec. in each parameter was obtained. This iteration was necessary because the partial derivatives used are all functions of $A_{\rm c}$, $B_{\rm c}$, $C_{\rm c}$.

The observed and calculated quadrupole splittings are compared in Table III for the three vibrational states of 1,3,2-dioxaborolane. The experimental hypothetical unsplit frequencies for the observed transitions and the differences between these frequencies and those calculated from the rotational constants are listed in Table IV.

The three observed states were tentatively assigned as the ground and two excited vibrational states. The relative intensities decreased in order of increasing frequency of the 0 \rightarrow 1₁₁ transition. The assignment of the first spectrum as the ground state was confirmed by the fact that no similar transitions of greater intensity could be found within any reasonable range of frequency. The second state was

Observed and calculated frequency splittings (Mc/sec) of quadrupole hyperfine components for 1,3,2-dioxaborolane: parent species (the estimated experimental error is \pm .05 Mc/sec.) Table III.

		Ground State	State	First Exc	First Excited State	Second Excited State	ited State
Transition	Components	Observed Splitting	Calculated Splitting	Observed Splitting	Calculated Splitting	Observed Splitting	Calculated Splitting
0 -> 111	(3/2 -> 5/2) - (3/2 -> 3/2) (3/2 -> 5/2) - (3/2 -> 1/2) (3/2 -> 5/2) - (3/2 -> 1/2) (3/2 -> 3/2) - (3/2 -> 1/2)	+ .57 43 -1.00	+ .60 48 -1.08	+ .5. 14 14	+ .56 44 -1.00	+ .52 a	9. +
$1_{10} -> 2_{21}$	$(5/2 \rightarrow 7/2) - (3/2 \rightarrow 5/2)$	๗		69. +	99° +	+ .63	9. +
1 ₁₁ -> 2 ₀₂	$(5/2 \rightarrow 7/2) - (1/2 \rightarrow 3/2)$	æ		+ .57	9.	+ .68	<i>-</i> 4.67
101 -> 212	$(5/2 \rightarrow 7/2) - (3/2 \rightarrow 5/2)$	+ .54	+ .53	+ .54	+ .50	๗	
202 -> 211	$(7/2 \rightarrow 7/2) - (5/2 \rightarrow 5/2)$ $(7/2 \rightarrow 7/2) - (1/2 \rightarrow 1/2)$ $(5/2 \rightarrow 5/2) - (1/2 \rightarrow 1/2)$	-1.33 +1.00 +2.33	-1.26 +1.02 +2.28	તા તા તા		-1.32 a a	-1.31
2 ₁₂ -> 2 ₂₁	$(7/2 \rightarrow 7/2) - (5/2 \rightarrow 5/2)$ $(7/2 \rightarrow 7/2) - (1/2 \rightarrow 1/2)$ $(5/2 \rightarrow 5/2) - (1/2 \rightarrow 1/2)$	в в	. 88	80 80	79	79 + .66 +1.45	80 + .66 +1.46
312 -> 321	$(9/2 \rightarrow 9/2) - (7/2 \rightarrow 7/2)$	ಡ		ช		69	65
c							

asplittings not resolved.

Table IV. Experimental hypothetical unsplit frequencies (Mc/sec) assigned for 1,3,2-dioxaborolane: parent species (the estimated experimental error is \pm .03 Mc/sec.)

	Ground S	State	First Excited State		Second Excited State	
Transition	Exp. Frequency	Exp Calc.	Exp. Frequency	Exp Calc.	Exp. Frequency	Exp Calc.
0 -> 1 ₁₁	12,638.11	+.05	12,665.40	+.03	12,670.74	+.06
1 ₁₀ -> 2 ₂₁	29,409.59	+.01	29,446.18	03	29,449.91	05
1 ₁₁ -> 2 ₀₂	20,403.38	+.05	20,484.28	+.01	20,503.30	+.11
1 ₀₁ -> 2 ₁₂	21,142.64	02	21,215.26	01	21,232.82	+.06
2 ₀₂ -> 2 ₁₁	10,518.89	02	10,484.20	+.03	10,467.19	+.06
2 ₁₂ -> 2 ₂₁	12,400.35	03	12,346.45	+.04	12,325.82	+.02
2 ₀₂ -> 3 ₁₃	29,354.16	04	29,474.96	+.01	29,505.18	+.01
2 ₁₂ -> 3 ₀₃	29,263.23	02	29,385.54	06	29,415.96	06
3 ₁₂ -> 3 ₂₁	a		a		9,873.29	06

aTransition not measured.

assigned a quantum number of 1 for a low frequency vibration. A larger quantum number was not likely, due to the high population deduced from the intensity relative to the ground state. The third state obviously was a still higher vibrational state, and was felt to be the v=2 level of the same normal mode. The fact that the three states lay in a series of decreasing intensity, and that no other excited states could be located, gave some foundation to the v=2 assignment for the third state. The possibility that it was the v=1 state of a different normal mode could not be excluded at this time, however.

The spectra of three isotopically substituted species of 1,3,2-dioxaborolane were also examined. These were the 4,4,5,5-tetradeutero, (referred to as 4-D), the ¹³C, and the ¹⁰B species. The rotational spectrum was predicted for each of these by first performing the isotopic substitution in the assumed trial structure. From this the second moments of inertia were calculated. The calculated second moments were improved by employing the observed second moments for the parent molecule in equations of the form

$$P_{\alpha\alpha}(isotope, predicted) = P_{\alpha\alpha}(isotope, calculated) + (4-3)$$

$$[P_{\alpha\alpha}(parent, observed) - P_{\alpha\alpha}(parent, calculated)].$$

The rotational constants corresponding to these predicted second moments were then used to compute a predicted rotational spectrum. The analysis of each spectrum then followed the procedure outlined for the parent species. These analyses were simpler than that for the parent since it was possible to limit the range in which the spectral parameters could

be expected to be found. The experimental rotational constants for each species were generally found to be within 20 or 30 Mc/sec. of the predicted values. This meant that the desired transitions could be located rather easily, close to the predicted frequencies. Comparisons with the parent transitions of Stark effects, quadrupole splittings, and line shapes were also of great help. Finally, the first excited vibrational state served as an aid rather than a complication in analyzing the substituted spectra, since now at least two similar transitions were expected in each region.

For the 4-D species, rotational transitions for three vibrational states were observed. The relative intensities decreased in order of increasing frequency of the 0 \rightarrow 1₁₁ transition, as they had in the parent. The states were tentatively assigned v = 0, 1, and 2 for the low frequency vibrational mode. The possibility that the third state had v = 1 for a different vibrational mode could not yet be excluded in this case, as it could not in the parent. Some transitions which might be due to a fourth vibrational state were observed, but it was not possible to locate a sufficient number of them to confidently determine a set of rotational constants.

The observed and calculated quadrupole splittings are compared in Table V for the three vibrational states of the 4-D species. The experimental hypothetical unsplit frequencies and the differences between these and the frequencies claculated from the rotational constants are listed in Table VI.

An estimate of the magnitude of centrifugal distortion effects may be made by comparing the frequencies of the 0 -> 1_{11} and 2_{11} -> 3_{22}

Observed and calculated frequency splittings (Mc/sec) of quadrupole hyperfine components for 1,3,2-dioxaborolane: $\mu,\mu,5,5$ -tetradeutero- species (the estimated experimental error is \pm .05 Mc/sec.) Table V.

		Ground State	State	First Exc	First Excited State	Second Ex	Second Excited State
Transition	Components	Ob s erved S pli tting	Calculated Splitting	Observed Splitting	Calculated Splitting	Observed Splitting	Calculated Splitting
0 -> 111	$(3/2 \rightarrow 5/2) - (3/2 \rightarrow 3/2)$ $(3/2 \rightarrow 5/2) - (3/2 \rightarrow 1/2)$ $(3/2 \rightarrow 5/2) - (3/2 \rightarrow 1/2)$ $(3/2 \rightarrow 3/2) - (3/2 \rightarrow 1/2)$	+ .53 44 97	+ .56 45 -1.01	+ .59 46 -1.05	+ .60 148 -1.08	+ :53	55: + 144: - 199: -
$1_{10} \rightarrow 2_{21}$	$(5/2 \rightarrow 7/2) - (3/2 \rightarrow 5/2)$ $(5/2 \rightarrow 7/2) - (1/2 \rightarrow 3/2)$ $(3/2 \rightarrow 5/2) - (1/2 \rightarrow 3/2)$	+ .63 52 -1.15	+ .56 59 -1.15	+ % a a	09.	៧ ៧ ៧	
$1_{11} -> 2_{02}$	$(5/2 \rightarrow 7/2) - (1/2 \rightarrow 3/2)$	+ .50	+ .50	ď		+ .44	+ .48
$1_{01} -> 2_{12}$	(5/2 -> 7/2) - (3/2 -> 5/2)	75. +	+ .56	+ .55	+ .55	.50	+ .47
202 -> 211	(7/2 -> 7/2) - (5/2 -> 5/2)	-1.31	-1.26	-1.29	-1.22	๙	
2 ₁₂ -> 2 ₂₁	$(7/2 \rightarrow 7/2) - (5/2 \rightarrow 5/2)$ $(7/2 \rightarrow 7/2) - (1/2 \rightarrow 1/2)$ $(5/2 \rightarrow 5/2) - (1/2 \rightarrow 1/2)$	80 + .62 +1.42	79 + .63 +1.42	78 + .60 +1.38	78 + .62 +1.39	75 + .51 +1.26	72 + .55 +1.26
2 ₁₁ -> 3 ₂₂	(7/2 -> 9/2) - (5/2 -> 7/2)	+ .59	+ .58	๗		٠ + 6	+ .50

Splitting not resolved.

Table VI. Experimental hypothetical unsplit frequencies (Mc/sec) assigned for 1,3,2-dioxaborolane: 4,4,5,5-tetradeuterospecied (the estimated experimental error is ± .03 Mc/sec.)

	Ground S	State	Fir s Excited		Seco Excited	
Transition	Exp. Frequency	Exp Calc.	Exp. Frequency	Exp Calc.	Exp. Frequency	Exp Calc.
0 -> 1 ₁₁	10,904.60	+.03	10,927.61	01	10,932.57	+.10
1 ₁₀ -> 2 ₂₁	25,076.57	02	25,105.83	03	25,110.02	03
1 ₁₁ -> 2 ₀₂	18,243.16	+.06	18,314.95	06	18,331.62	10
1 ₀₁ -> 2 ₁₂	18,541.68	01	18,604.65	+.03	18,619.87	+.04
2 ₀₂ -> 2 ₁₁	8,981.59	+.01	8,954.14	+.03	8,941.56	+.08
2 ₁₂ -> 2 ₂₁	9,802.36	01	9,751.89	+.03	9,735.27	06
2 ₀₂ -> 3 ₁₃	26,046.31	+.02	26,152.71	+.01	26,178.92	+.03
2 ₁₂ -> 3 ₀₃	26,026.70	05	26,134.21	.00	26,160.52	03
2 ₂₁ -> 3 ₁₂	31,780.96	03	31,878.96	04	31,898.29	04
2 ₁₁ -> 3 ₂₂	32,713.54	17 ^a	32,782.69	17 ^a	32.797.24	17 ^a

anot included in the rigid rotor fitting.

transitions. For an undistorted rigid rotor $3v_0 \rightarrow 1_{11} = v_{2_{11}} \rightarrow 3_{22}$. The observed $2_{11} \rightarrow 3_{22}$ transitions are .24 to .47 Mc/sec. lower than the values of $3v_{0\rightarrow 1_{11}}$. This demonstrates that some centrifugal distortion is present but that the effects are small enough to be ignored in the present analysis.

For the ¹³C species rotational transitions for two vibrational states were observed, corresponding to the ground and lower excited states found for the parent and 4-D species. It was not possible to locate transitions for the third vibrational state, nor to measure the transitions as accurately as for the other two species, because the 13C sample decomposed a few days after it was first examined in the spectrometer. Water or some other impurity had been admitted to the sample tube either by leakage through the stopcock during the 14 months that the sample had been stored, or directly from the spectrometer vacuum system. Each time the sample was warmed to introduce it into the absorption cell, a substantial amount of non-condensable gas was released. The sample was vacuum distilled in an attempt to eliminate the decomposition, but this was only partially successful. It was possible to measure enough transitions to determine the two sets of rotational constants, but a greater error must be expected in these than in the parent and 4-D constants.

The observed and calculated quadrupole splittings are compared in Table VII for both vibrational states of the ¹³C species. The experimental hypothetical unsplit frequencies and the differences between these and the frequencies calculated from the rotational constants are listed in Table VIII.

Table VII. Observed and calculated frequency splittings (Mc/sec) of quadrupole hyperfine components for 1,3,2-dioxaborolane: ^{13}C species. (The estimated experimental error is \pm .10 Mc/sec.)

		Ground	State		rst 1 State
Transition	Component s	Ob s. S pli t- ting	Calc. Split- ting	Ob s. S pli t- ting	Calc. Split- ting
0->111	$(3/2 \rightarrow 5/2) - (3/2 \rightarrow 3/2)$ $(3/2 \rightarrow 5/2) - (3/2 \rightarrow 1/2)$ $(3/2 \rightarrow 3/2) - (3/2 \rightarrow 1/2)$	+ .57 44 -1.01	+ .57 45 -1.02	+ .55 a a	+ .60
1 ₁₁ ->2 ₀₂	(5/2-3/2)-(3/2-31/2) (5/2-3/2)-(1/2-3/2)	+ .62	+ .61	+ .65	+ .63
2 ₁₂ ->2 ₂₁	(7/2->7/2)-(5/2->5/2)	87	88	84	85
3 ₁₂ ->3 ₂₁	(9/2 - >9/2)-(7/2 - >7/2)	60	59	66	61

asplitting not resolved

Table VIII. Experimental hypothetical unsplit frequencies (Mc/sec) assigned for 1,3,2-dioxaborolane: 13 C species. (The estimated experimental error is \pm .08 Mc/sec.)

	Ground S	tate	Fi rs t Excited	State
Transition	Experimental Frequency	Exp Calc.	Experimenta1 Frequency	Exp Calc.
0 -> 111	12,474.99	+ .12	12,501.91	+ .04
1 ₁₀ -> 2 ₂₁	29,025.44	05	29,061.45	06
1 ₁₁ -> 2 ₀₂	20,169.85	24	20,250.89	+ .01
1 ₀₁ -> 2 ₁₂	20,873.97	02	20,945.73	24
2 ₁₂ -> 2 ₂₁	12,227.24	01	12,173.41	+ .10
2 ₀₂ -> 3 ₁₃	28,992.03	+ .16	a	
2 ₁₂ -> 3 ₀₃	a		29,029.83	+ .15
3 ₁₂ -> 3 ₂₁	9,842.74	+ .07	9,813.24	03

a Transition not measured.

For the ¹⁰B species rotational transitions for the ground vibrational state were observed. The observed and calculated quadrupole splittings and the experimental hypothetical unsplit frequencies and the differences between these and the frequencies calculated from the rotational constants, are listed in Table IX. The larger quadrupole moment of the ¹⁰B nucleus caused greater splittings than for the other species, although the values were still small.

The values of the rotational constants, principal moments of inertia, and second moments of inertia for each of the species of 1,3,2-dioxaborolane which was examined, are presented in Table X. The values of the quadrupole coupling constants are listed in Table XI.

4.4 Discussion of the Bond Characters

Information on the electron distribution in 1,3,2-dioxaborolane may be obtained from calculations based on the experimental values of the quadrupole coupling constants. These calculations will provide an estimate of the non-localized and polar characters of the B-O and B-H bonds. The results of the following calculations, which make use of the ideas of Townes and Dailey (22), must be considered as no more than estimates due to the number of simplifying assumptions which will be invoked.

To start, the orbitals used by the boron atom to form its σ bonds are taken to be

$$\Psi_1 = 1/\sqrt{3} \text{ (S} + \sqrt{2} P_y)$$
 B-H bond,
 $\Psi_2 = 1/\sqrt{3} \text{ (S} + \sqrt{6/2} P_x - \sqrt{2/2} P_y)$ B-O bond, (4-4)
 $\Psi_3 = 1/\sqrt{3} \text{ (S} - \sqrt{6/2} P_x - \sqrt{2/2} P_y)$ B-O bond.

Table IX. Observed and calculated frequency splitting (Mc/sec) of quadrupole hyperfine components, and experimental hypothetical unsplit frequencies (Mc/sec) assigned for 1,3,2-dioxaborolane: ¹⁰B species.

Transition	Component s	Obs. Split- ing	Calc. Split- ing	Exp. Huf ^c	Exp Calc.
0 -> 1 ₁₁	$(3 \rightarrow 4) - (3 \rightarrow 3)$ $(3 \rightarrow 4) - (3 \rightarrow 2)$ $(3 \rightarrow 3) - (3 \rightarrow 2)$	40	43	12,883.35	02
1 ₁₀ -> 2 ₂₁	$(4 \rightarrow 5) - (3 \rightarrow 4)$ $(4 \rightarrow 5) - (2 \rightarrow 3)$ $(3 \rightarrow 4) - (2 \rightarrow 3)$	68	62	30,046.23	+ .02
1 ₁₁ -> 2 ₀₂		a		20,496.04	05
1 ₀₁ -> 2 ₁₂	(4 -> 5) - (3 -> 4)	+1.05	+1.06	21,487.28	+ .01
2 ₁₂ -> 2 ₂₁	(5 -> 5) - (4 -> 4)	-1.28	-1.36	12,838.38	03
2 ₀₂ -> 3 ₁₃		a		29,724.10	+ .04
2 ₁₂ -> 3 ₀₃		a		29,569.69	+ .02
3 ₁₂ -> 3 ₂₁	(6 -> 6) - (5 -> 5)	96	97	9,778.73	+ .02

^aNo splitting resolved.

 $^{^{\}rm b}$ The estimated experimental error is \pm .05 Mc/sec.

 $^{^{\}rm C}$ The estimated experimental error is \pm .03 Mc/sec.

Rotational constants (Mc/sec), principal moments of inertia $(AMU-A^2)^a$, and second moments of inertia $(AMU-A^2)^b$ for 1,3,2-dioxaborolane Table X.

		A	B	υ	H	'I I	Ī	P.,	٦. ۲.	ا م
					ਹ	q	υ		aa	ပ
OCH 2CH 20BH	Ground State	8385.76 ^c	7730.56 ^c	4252,30 ^c	60.28446	65.39384	8385.76 ^c 7730.56 ^c 4252.30 ^c 60.28446 65.39384 118.88413 61.99676 56.88738 3.39708	61.99676	56.88738	3.39708
	First Excited State	8390.42 ^c	7742.11 ^C	4274.95°	60.25098	65.29628	8390.42 ^c 7742.11 ^c 4274.95 ^c 60.25098 65.29628 118.25425 61.64978 56.60447 3.64651	61.64978	56.60447	3.64651
Ħ	Second Excited State		7742.58 ^d	4281.04 ^c	60.25658	65.29232	8389.64° 7742.58 ^d 4281.04° 60.25658 65.29232 118.08603 61.56088 56.52514 3.73144	61.56088	56.52514	3.73144
OCD2CD2OBH	Ground State	7086.01 ^{°C}	6806.17 ^C	3818.56°	71.34212	74.27540	7086.01 ^c 6806.17 ^c 3818.56 ^c 71.34212 74.27540 132.38786 67.66057 64.72729 6.61483	67.66057	64.72729	6.61483
ш	First Excited State		6817.28 ^c	3838.50 ^c	71.31083	74.15436	6817.28 ^c 3838.50 ^c 71.31083 74.15436 131.70014 67.27184 64.42831 6.88252	67.27184	64.42831	6.88252
Ŧ	Second Excited State	7088.79°		3843.68 ^c	71.31415	74.14326	6818.30 ^d 3843.68 ^c 71.31415 74.14326 131.52266 67.17589 64.34677 6.96738	67.17589	64.34677	6.96738
013CH ₂ CH ₂ OBH Ground State	H Ground State	8275.31 ^d	7649.16 ^e	4199.56 ^d	8275.31 ^d 7649.16 ^e 4199.56 ^d 61.08907 66.08974	72680.99	120.37713 62.68890 57.68823 3.40084	62,68890	57.68823	3.40084
E	First Excited State	8279.82 ^d	7660.97 ^e	4222.05 ^d	7660.97 ^e 4222.05 ^d 61.05580 65.98786	65.98786	119.73591 62.33399 57.40192 3.65387	62.33399	57.40192	3.65387
OCH2CH2010BH		8581.42 ^c	7730.04 ^d	4301.95°	58.90995	65.39824	8581.42 ^c 7730.04 ^d 4301.95 ^c 58.90995 65.39824 117.51206 62.00018 55.51188 3.39806	62,00018	55.51188	3.39806
מ	;		Q2 mg /	p1	1 2 2 2 1 1 2 2	0) == ====	M / brainstant to 0 CR + 1 CR +			

^CEstimated uncertainty is ^eEstimated uncertainty is \pm .05 Mc/sec. ^DCalculated by equation (2-9). dEstimated uncertainty is ± .03 Mc/sec. Conversion factor $505531 \text{ AMU-}R^2 - \text{Mc/sec.}$ ± .02 Mc/sec.

Table XI. Quadrupole coupling constants (Mc/sec) for 1,3,2-dioxaborolane

) aa	$\chi_{ t bb}$	Xcc
OCH ₂ CH ₂ OBH	Ground State	67 ^a	-2.41 ^a	+3.08 ^a
<u> </u>	First Excited State	58ª	-2.23 ^a	+2.81ª
	Second Excited State	50 ^b	-2.40 ^a	+2.90 ^a
OCD ₂ CD ₂ OBH	Ground State	53 ^a	-2.24ª	+2.77 ^a
	First Excited State	42 ^b	-2.41 ^b	+2.83 ^b
	Second Excited State	37 ^b	-2.20 ^b	+2.57 ^b
O ¹³ CH ₂ CH ₂ OBH	Ground State	72 ^b	-2.26 ^b	+2.98 ^b
	First Excited State	60 ^b	-2.41 ^b	+3.01 ^b
OCH ₂ CH ₂ ¹⁰ BH		∞ ^b	-6.09 ^a	+6.99ª

^aEstimated uncertainty ± .10 Mc/sec.

bEstimated uncertainty ± .20 Mc/sec.

The gradient of the field at the B nucleus is then assumed to be expressible in equations of the form,

$$q_{\alpha} = [U_{\alpha} - 1/2(U_{\beta} + U_{\gamma})]q_{0}$$
, with (4-5)

 U_{α} = number of P electrons in the valence P_{α} orbital (α , β , γ are mutually perpendicular),

and q_0 = contribution of one valence P electron to q_α .

It is found that assuming non-polar bonds, with or without π bonding leads to the constraint $q_x = q_y$. This is contrary to the experimental result that

$$eQq_x = \chi_{aa} = -0.67 \text{ Mc/sec.},$$
 $eQq_y = \chi_{bb} = -2.41 \text{ Mc/sec.},$
 $eQq_z = \chi_{cc} = +3.08 \text{ Mc/sec.}$

Therefore it is necessary to assume a polar character to some of the bands to boron. The electronegativity values (B = 2.0, O = 3.5, H = 2.2) suggest assuming that the B-O bonds are polar, with the oxygen more electronegative than the boron.

Therefore n_p electrons per B-O bond are assumed to have been transferred from the boron orbitals to the oxygens. Of these electrons, 1/6 per bond are P_y and 1/2 per bond are P_x . The contributions to U_x are then

+ 1/2 electron from each of Ψ_2 and Ψ_3 , and $-2(\frac{n_p}{2})$ electrons "lost" to the oxygens.

The contributions to $\textbf{U}_{_{\boldsymbol{V}}}$ are

- + 2/3 electron from Ψ_1 ,
- + 1/6 electron from each of Ψ_2 and Ψ_3 , and $-2(\frac{n_p}{6})$ electron lost to the oxygen.

The only contribution to \mathbf{U}_z is from \mathbf{n}_r electrons contributed to the boron \mathbf{P}_z orbital from the occupied \mathbf{P}_z orbitals on the oxygens. Therefore,

$$U_{x} = 1 - n_{p}$$
,
 $U_{y} = 1 - 1/3 n_{p}$, (4-6)
 $U_{z} = n_{\pi}$,

and

$$\begin{aligned} & \text{eQq}_{\text{X}} = (1/2 - 5/6 \, \text{n}_{\text{P}} - 1/2 \, \text{n}_{\text{T}}) \text{eQq}_{\text{O}} = -.67, \\ & \text{eQq}_{\text{y}} = (1/2 + 1/6 \, \text{n}_{\text{P}} - 1/2 \, \text{n}_{\text{T}}) \text{eQq}_{\text{O}} = -2.41, \\ & \text{eQq}_{\text{z}} = (-1 + 2/3 \, \text{n}_{\text{P}} + \text{n}_{\text{T}}) \text{eQq}_{\text{O}} = +3.08. \end{aligned} \tag{4-7}$$

Solving these gives

$$n_p = -1.74/eQq_0,$$

 $n_{\pi} = 1 + 4.24/eQq_0.$

If eQq_0 is assumed to be -5.3 (31), these become

$$n_{p} = .33,$$
 $n_{rr} = .20.$

The number of "boron electrons" from the B-O bond wave function,

 $\Phi_{\rm BO} = [\Psi_{\rm B} + \lambda \, \Psi_{\rm O}][1 + \lambda^2]^{-1/2}$, is $2/(1 + \lambda^2)/$ This is equal to $1 - n_{\rm p}$, so $\lambda^2 = 2.0$ and the ionic character of the B-O bond, $(\lambda^2 - 1)/(\lambda^2 + 1)$, is 0.33. The value of $n_{\rm H}$ indicates that the π bonding system has about a 10% contribution to the electronic structure.

Some polar character to the B-H bond may be assumed, with H more negative than B. For a B-H bond of 10% ionic character, the B-O bond ionic character changes from 33% to 43% and the π bonding contribution decreases to 5%

The stability and monomeric nature of 1,3,2-dioxaborolane has been attributed in a large part to the formation of B-O π bonds (32). To retain some π bonding in the above scheme, it is necessary to deny that there is much ionic character in the B-H bond.

4.5 Determination of the Molecular Symmetry and Structure

Once the rigid rotor and quadrupole analyses had been completed the molecular structure and the vibrational effects could be examined in detail. The three most likely configurations of the heavy atoms were a planar ring with C_{2V} symmetry, a symmetrically staggered ring with C_2 symmetry, and a boat or bowl form with σ_h ($C_{1h} \equiv C_s$ group) symmetry.

Relative intensity measurements were expected to help discriminate between the types of symmetry, since the C_{2V} and C_2 symmetries could produce effects of nuclear spin statistics while the σ_h symmetry could produce no such effect. Furthermore, the relative intensities of the same rotational transition in different vibrational states would provide an estimate of differences in vibrational energy of these states.

A second test of the symmetry was the principal axis orientation of the dipole moment. In all three cases the major component of μ_D was expected to be along the b "symmetry" axis with a zero component along the a axis, across the ring. The c component (perpendicular to the ring) would vanish for C_{2V} and C_2 symmetries but should be non-zero for the σ_h symmetry.

A third test of the symmetry was the geometrical coordinates of the B atoms. The a coordinate should be zero in all three cases. The c coordinate must also be zero for the C_{2V} and C_2 symmetries, but should be finite for σ_h symmetry.

The indicated experiments were then performed in order to establish the symmetry of the molecular configuration.

a) Relative Intensities of Absorption Transitions

The absolute intensity of a rotational transition is a function of many factors. The relative transition intensities, however, for a given sample at constant temperature, pressure, microwave power and for reasonably close frequencies may be expressed far more simply, as

$$I_r = S_r f_v g_n, \qquad (4-8)$$

where \mathbf{S}_{r} is the relative rotational line strength and may be calculated once the rotational constants and dipole moment are known, \mathbf{f}_{v} is the fractional population of the vibrational state concerned

$$f_v = g_v e^{-E_V/kT}$$

and \boldsymbol{g}_{n} is the relative nuclear spin statistical weight.

The nuclear spin statistical weight is necessarily included only if the molecule is symmetric to a 180° rotation about a principal axis. The appropriate g_n is calculated by determining the number of nuclear spin wave functions which combine with the vibration-rotation wave functions to produce the correct symmetry to the C_2 operations. For an interchange of n pairs of identical nuclei of spin I_i the number of symmetric spin functions which may be constructed is (31)

$$n_{\text{symm}} = 1/2 \begin{bmatrix} n \\ i = 1 \end{bmatrix} (2I_i + 1) \begin{bmatrix} n \\ i = 1 \end{bmatrix} (2I_i + 1) + 1,$$
 (4-9)

and the number of antisymmetric functions is

$$n_{\text{antisymm}} = 1/2 \begin{bmatrix} n \\ \pi \\ i = 1 \end{bmatrix} (2I_i + 1) \begin{bmatrix} n \\ \pi \\ i = 1 \end{bmatrix} (2I_i + 1) - 1 \end{bmatrix}.$$
 (4-10)

For 1,3,2-dioxaborolane a rotation about the b axis may interchange 2 pairs of hydrogens of spin 1/2 (also 1 pair of carbons and 1 pair of oxygens, but their spins of zero do not contribute). The ratio of the number of symmetric to antisymmetric functions in this case is 5:3. When 4 deuteriums (I = 1) are substituted for the hydrogens, the symmetric to antisymmetric ratio becomes 5:4. In both cases the total wave function must be symmetric to the interchange.

The symmetry of a given vibration-rotational level is the product of the rotational symmetry and the vibrational symmetry. Wilson, Decius, and Cross (33) demonstrate the following statements for vibrational wave functions:

- 1) The ground vibrational state is totally symmetric.
- 2) An excited state of a non-degenerate normal mode is totally symmetric for even values of the quantum number.
- 3) An excited state of a non-degenerate normal mode has the same symmetry as the normal coordinate for odd values of the quantum number.
- 4) Excited states of degenrate vibrations have a combination of wave functions, with more than one symmetry species represented.

The symmetry of a vibrational state with respect to the C_2 operation may be determined by measuring the relative intensities of two rotational transitions which have initial rotational levels of opposite symmetry. The relative statistical weights are then equal to the relative intensities corrected by the rotational line strength factor. Finally, by recognizing which statistical weight corresponds to the symmetric initial rotational level, the vibrational symmetry may be deduced.

b) Intensity Measurements

The accurate measurement of intensities is still a major problem in microwave spectroscopy. Data on vibrational frequencies, barriers to internal rotation, conformational isomers, quantitative analysis etc., and the analysis of spectra in general could be much improved by more precise methods. Even with the relatively large uncertainties presently involved, however, it is possible to obtain useful information from relative intensity measurements.

The most important single difficulty probably is caused by reflections of the microwave radiation within the system. These can lead to an effective sample path length which is both unknown and highly frequency dependent. Reflections also cause standing waves which can make the detection process highly frequency dependent. To minimize reflections use is made of tapered transitions between sections of the waveguide, thin mica windows on the absorption cell, attenuators, and isolation units (in which attenuation in one direction is many times that in the opposite direction). Other problems

encountered are ground loops, pickup, non-linear detection and amplification, variations in microwave power, and interference from nearby transitions.

In measuring relative intensities for transitions of 1,3,2-dioxaborolane and the 4-D species it was hoped that the problems listed above could be minimized if the following procedure was used. Comparable measurements were made at constant pressure with the wavequide cell at dry ice temperature, with the microwave power level held constant, with the crystal mount adjusted for maximum sensitivity, with the klystron source tuned until the desired frequency occurred at a flat portion of the mode, with constant sweep width, and with the Stark modulation voltage for comparable transitions adjusted to similar values consistent with the least interference from other transitions. The measurements on which the estimates of the vibrational energy levels are based were made with a ferrite isolator between the absorption cell and the detector. The absolute intensities were found to decrease with increasing length of time after introducing the sample into the cell. To minimize the effect of this variation of intensity with time, the reported measurements were made after the sample had been in the cell 2 or more hours, and an average was taken over a series of measurements, alternating between the lines being compared.

The transitions measured include both symmetric and antisymmetric initial rotational levels for each vibrational level. The choice of transitions was made on the basis of proximity of frequency and likelihood of oscilloscope display. Tables XII and XIII list

Table XII. Relative intensity of the $(2_{12} -> 3_{03})$ to the $(2_{02} -> 3_{13})$ transitions in 1,3,2-dioxaborolane.

	Ground State	Fir s t Excited State	Second Excited State
Measurement (1)	. 55	.89	.76
(2)	.68	.74	.60
Average	<.62>	<.81>	<. 68>
Expected a	. 598	.598	.598
b	1.672	1.672	1.672
С	•997	•997	• 997

For vibrational state symmetric to C₂^b.

Table XIII. Relative intensity of the $(3_{03} -> 4_{14})$ to the $(3_{13} -> 4_{04})$ transitions in tetradeutero-1,3,2-dioxaborolane.

	Ground State	First Excited State
Measurement (1)	.74	.74
(2)	.85	.74
Average	<. 79>	<.74>
Expected	80	80
a b	.80 1.25	.80 1.25
c	1.00	1.00

For vibrational state symmetric to C₂^b.

 $^{^{\}rm b}$ For vibrational state antisymmetric to ${\rm C_2}^{\rm b}$.

CFor no C₂ b symmetry.

^bFor vibrational state antisymmetric to C₂^b.

^cFor no C₂ symmetry.

relative intensities for transitions of the two symmetries to C_2^b within each vibrational state. The $3_{03} \rightarrow 4_{14}$ and $3_{13} \rightarrow 4_{04}$ transitions for the 4-D species are particularly convincing, since in each vibrational state they were separated by less than 1 Mc/sec. and were measured simultaneously on the oscilloscope. It was unfortunate that the same transitions for the second excited state occurred in a frequency region which was inaccessible because of klystron failure.

In each case the rotational level which is symmetric to C_2^b is stronger than the level antisymmetric to C_2^b by an amount similar to that predicted. The conclusion is that 1,3,2-dioxaborolane possesses at least a C_2^b axis of symmetry. Furthermore all three vibrational states have a wave function symmetric to this rotation. Other evidence to support these conclusions will be derived from the dipole moment orientation and the effective structure.

In order to estimate the difference in vibrational energy between the ground and excited states, the relative intensities of several corresponding rotational transitions in each vibrational state were measured. The intensities are listed in Table XIV relative to the ground state transition. The vibrational energy differences were calculated with the relation

$$\frac{I_{v}}{I_{o}} = e^{-(E_{v}-E_{o})/kT}$$
, with kT/hc = 135.5 cm⁻¹. (4-11)

These measurements demonstrate clearly that both the first and second excited states' vibrational wave functions are symmetric to $C_2^{\ b}$.

They further show that the vibrational mode has quite a low frequency, and that the frequency is markedly decreased on substituting deuterium for the methylene hydrogen atoms.

Table XIV. Relative intensities of rotational transitions and estimated vibrational energies (cm^{-1}) .

	Ground	Fir s t	Excited	State	Second	Excited	State
Transition	State Re1. Int.	Rel. Int.	E_1-E_0 a	E_1-E_0	Re1. Int.	E ₂ -E ₀ a	E ₂ -E ₀
$\frac{1,3,2-\text{Dioxaboro}}{3_{12}} \rightarrow 3_{21}$ (1)	1.0	.68	52	-18	.53	86	16
(2)	1.0	.64	60	-10	.51	91	22
2 ₀₂ -> 2 ₁₁	1.0	.64	60	131	.49	96	167
O ₀₀ -> 1 ₁₁	1.0	.73	42	111	.56	78	146
Average $(E_V^{-E_0})$			53±15			8 8 ±20	
4-D-1,3,2-Dioxal	orolane						
3 ₂₂ -> 3 ₃₁	1.0	.85	22	52	.54	83	114
$0_{00} \rightarrow 1_{11} (1)$	1.0	.87	19	48	.67	54	83
(2)	1.0	.84	24	54	.64	60	91
Average $(E_v - E_0)$			22±10			66±20	

aEnergy difference (cm $^{-1}$) calculated assuming vibration symmetric to C_2^b .

^bEnergy difference (cm^{-1}) calculated assuming vibration antisymmetric to $C_2^{\ b}$.

C) Determination of the Dipole Moment

The dipole moment components were determined for the parent species by measuring the frequency shift of some absorption transitions at each of several values of the applied Stark field. This was accomplished by applying a high D.C. voltage through a calibrated voltage divider to bias the square wave generator output above ground potential. The voltage settings were converted to values of the electric field by calibration with the known Stark shift of the OCS O -> 1 transition at 12,162.99 Mc/sec.

There is a problem concerning the value of the OCS dipole moment to be used in the equation for the known Stark effect. The best value for μ_{D} was obtained by Marshall and Weber (34). They used sufficiently large field strengths to observe the second and fourth order field effects of μ_{D}^{2} and μ_{D}^{4} and the effect of the second order polarizability perturbation. Their "true" value of μ_D was 0.7124 ± .0002 D. Previously Shulman and Townes (10) had measured the Stark effect at lower field strengths and obtained an effective dipole moment of 0.7085 D. The only concern here with the value of μ_D is that it is presently necessary to use it to calculate the OCS Stark effect. The problem could be circumvented by recognizing that OCS is simply a convenient laboratory standard, which is being employed to determine the effective electrode spacing in the waveguide cell which was used for the present work. Therefore, a table of frequency shifts versus known values of applied electric field, in a range of fields commonly used, would be more useful and less subject to debate than the determination of true or effective values for the OCS dipole moment.

Consideration was given to preparing a table of Δ_V versus E^2 from the data of Marshall and Weber and of Shulman and Townes, but the former did not report Δv versus E^2 directly and both pairs of workers obtained their Stark fields in a different manner from that used here. In order to decide which value of $\boldsymbol{\mu}_{D}$ is appropriate for the calibration, the contributions to the Stark shift from the polarizability and from the term in $\mu_{\text{D}}^{\boldsymbol{4}}$ were calculated, using the equations and experimental values reported by Marshall and Weber. This was done for a field strength of 6 statvolts/cm., which is approximately the maximum field strength which was achieved in the present work. The contribution due to the polarizability was entirely negligible; the contribution due to the μ_D^4 term was .016 Mc/sec., which is comparable to the estimated uncertainty (.02 Mc/sec.) for the measured frequencies, and which is 0.3% of the Stark shift calculated from the term in μ_D^2 . It was therefore decided to use μ_D = 0.7124 as the effective OCS dipole moment, since this is the most accurate value available, and since no effects from the higher order terms could have been observed at the field strengths used here.

The values of the OCS Stark shift were measured here with the un-calibrated cell, plotted against the square of the voltage settings, and fit to a straight line by least squares. The theoretical slope of this line divided by the experimental slope yielded a calibration constant k. The least squares slopes of similar plots for 1,3,2-dioxaborolane were then multiplied by k to obtain values of $\frac{d}{d} \frac{\Delta v}{(E^2)}$. The experimental error is believed to be less than 1%, since values of Δv from about 1.0 Mc/sec. to 8.0 Mc/sec. were measured with an estimated error in each measurement of less than ±.04 Mc/sec.

An equation for $\int \Delta v/\int (E^2)$ may be derived by taking the difference in the Stark energies (Equation 2-30) for the energy levels in the transition, inserting the proper value for $M(\Delta M=0)$ for the present experimental arrangement), differentiating with respect to E^2 , and noting that $(\Delta W_s) = v_{stark} - v_0$ is the Stark shift. Thus

$$\Delta W_{s} = W_{s}^{(2)} - W_{s}^{(1)} = E^{2} \left[\sum_{\alpha} (\Delta A_{\alpha} + \Delta B_{\alpha} M^{2}) \mu_{\alpha}^{2} \right],$$
 (4-12)

$$J(\Delta W_s)/J(E^2) = C_a \mu_a^2 + C_b \mu_b^2 + C_c \mu_c^2,$$
 (4-13)
 $C_a = \Delta A_a + \Delta B_a M^2, \text{ etc.}$

The coefficients C_a , etc. were calculated by the computer program EIGVALS. The components of μ_D were then determined by solving the linear system (or least squares system where there was a redundancy) for the Stark shifts of several transitions. Table XV lists the experimental values of $\partial \Delta v / \partial (E^2)$ and the C_a 's which were used.

Since it was of great interest to determine the c axis component of μ_D , the 2_{02} -> 3_{13} and 2_{12} -> 3_{03} transitions were measured. Both of these have large contributions to C_c from the near degeneracy of the 2_{02} and 2_{12} , and the 3_{13} and 3_{03} pairs of levels. The components of μ_D were calculated in four ways, all of which assumed μ_a = 0. (1) The linear system derived for transitions (A) and (B) was solved for μ_D^2 and μ_c^2 , (2) μ_D^2 and μ_C^2 were fit by least squares for the transitions listed as (A), (B), and (C), (3) μ_C^2 was assumed zero, and each of (A), (B), (C), and (D) was solved for the remaining μ_D^2 , (4) μ_C^2 was assumed = 0.0001, and each of (A), (B), (C), and (D) was solved for the remaining μ_D^2 . The results of these four calculations are listed in Table XVI.

Table XV. Data used in the dipole moment calculations.

Transition	Exp. _a Slope	91/9Esp	С _в	C _c
Ground State				
(A) $2_{02} \rightarrow 3_{13} M = 1$	+ 2.0404	0.17600	+0.0339401	+104.57881
(B) $2_{12} \rightarrow 3_{03} M = 1$	+ 1.2156	0.10485	+0.0199771	-104.55836
(C) $1_{01} \rightarrow 2_{12} M = 0$	+ 6.917	0.59664	+0.1143908	+ 0.0337893
(D) $1_{01} \rightarrow 2_{12} M = 1$	+40.54	3.496	+0.6578236	+ 16.937205
First Excited State				
$(A') 2_{02} -> 3_{13} M = 1$	+ 2.0548	0.17724	+0.0339338	+107.03608
(B') $2_{12} \rightarrow 3_{03} M = 1$	+ 1.2148	0.10479	+0.0200211	-107.01565
Second Excited State				
$(A'') 2_{02} -> 3_{13} M = 1$	+ 2.0235	0.17454	+0.0339675	+107.29849
(B") $2_{12} \rightarrow 3_{03} M = 1$	+ 1.1730	0.10118	+0.0200377	-107.27806

^aPractical units

 $^{^{\}rm b}$ 104 (Mc/sec)/(statvolt/cm)²

c₁₀₄ ((Mc/sec)/(statvolt/cm)²)/Debye²

Table XVI. Calculated dipole moment components (Debye²)

		Grou	nd State	First Ex	cited State	Second Ex	cited State
		$\mu_{\rm b}^{2}$	$\mu_{_{ m C}}^{2}$	μ_{D}^{2}	$\mu_{\rm C}^{\ 2}$	$\mu_{\rm b}^{\ 2}$	μ _C 2
(1)		5.2090	-7.6×10^{-6}	5.2271	-1.2x10 ⁻⁶	5.1054	+10.4×10 ⁻⁶
(2)		5.2151	$-8.0x10^{-6}$				
(3)	(A)	5.1856	0.0*	5.2231	o.o*	5.1385	0.0*
	(B)	5.2487	0.0*	5.2337	0.0*	5.0494	0.0*
	(C)	5.2159	0.0*				
	(D)	5.315	0.0*				
(4)	(A)	4.8775	0.0001*	4.9077	0.0001*	4.8226	0.0001*
	(B)	5.7719	0.0001*	5.7685	0.0001*	5.5849	0.0001*
	(C)	5.2158	0.0001*				
	(D)	5.312	0.0001*				

⁽¹⁾ Calculated by solving (A) and (B).

⁽²⁾ Calculated by least squares fit of (A),(B), and (C).

⁽³⁾ Calculated assuming μ_{c} = 0.0.

⁽⁴⁾ Calculated assuming $\boldsymbol{\mu}_{C}$ = 0.01.

^{*}Assumed value.

These calculations show that for all three vibrational states μ_{C} is certainly no larger than 0.01 D, and that it most probably is zero. The best values for $\mu=\left(\mu_{D}^{\ 2}\right)^{1/2}$ are $\mu_{V=0}=2.28\pm.02$ D, $\mu_{V=1}=2.29\pm.02$ D, $\mu_{V=2}=2.26\pm.02$ D. Thus, the dipole moments in all three vibrational states are equal within the estimated range of experimental error.

From the fact that μ_C vanishes, the structure with σ_h symmetry is highly unlikely, confirming the conclusions from the relative intensity measurements.

D) Boron Atom Coordinates and a Molecular Structure

The third evidence for C_2 (or C_{2V}) symmetry of the molecular configuration was the location of the boron atom. The coordinates of the boron atom were determined using the three Kraitchman equations (equation 2-45), and the experimental second moments of the ^{10}B and parent ground state species. The zero point vibration changed sufficiently with the ^{10}B substitution that the calculation of the a and c coordinates resulted in imaginary numbers. This result is precisely what is expected for an axial position of the substituted atom, and must be taken as evidence for the on-axis location of the B atom.

Thus, configuration with σ_h symmetry has been shown to be highly unlikely, in the light of the observation of the effects due to nuclear spin statistical weights, the dipole moment orientation, and the axial location of the B atom. The existence of at least C_2 symmetry is therefore well established. This symmetry was therefore invoked in determining the structure of 1,3,2-dioxaborolane. It

requires that $a_1 = -a_2$, $b_1 = b_2$, $c_1 = -c_2$ for the pair of oxygens, the pair of carbons, and the two pairs of methylene hydrogens (Hc).

There is not sufficient isotopic data to completely determine the molecular structure by the Kraitchman-Costain method. Only the coordinates of the boron and the two carbon atoms can be calculated from single substitution data. Once these coordinates are known, however, their contributions to the second moments of inertia and the center-of-mass equations can be subtracted. The B-H bond length was assumed to be 1.20 Å, so the contribution from this hydrogen can also be subtracted. Therefore, it remains to calculate the three coprdinates for the oxygen atom and six coordinates for the Hc's. Three Kraitchman type equations have been derived (Appendix B) for the 4-D substitution, subject to the C_2 symmetry condition. These result in one equation involving the b coordinates of two non-equivalent Hc's, and two mixed equations involving their a and c coordinates.

The b coordinates for the oxygen and for the two Hc's were determined from the equation for P_{bb} of the parent, from $\sum m_i b_i = 0$ for the parent, and from the 4-D Kraitchman-type equation for the hydrogen b coordinates. The three equations could not be satisfied simultaneously, with real values of the coordinates, since they were non-linear. A set of coordinates with minimal deviations did exist, however. This set was then chosen as yielding the "best" values for the three b coordinates, by adjusting them to satisfy both the 4-D substitution equation and the parent center of mass condition.

The a and c coordinates for the oxygen atom and for the methylene hydrogen atoms were then determined from the two equations for the parent P_{aa} and P_{cc} , the two Kraitchman-type equations in a_{H_1} , a_{H_2} , a_{H_2} , a_{H_2} , and the assumption that the methylene hydrogens are

each equally distant from the bonded carbon and equally distant from the non-bonded carbon. These two conditions are contained in the quite plausible assumption that the methylene angle is bisected by the O-C-C plane. It should be noted that a third constraint is implied by this bisection assumption, namely that both hydrogens be equally distant from the oxygen atom. This constraint was not used, since it was felt that if it were invoked errors in the O and H b coordinates would add large uncertainty to the a and c coordinates calculated. Indeed, when the six a and c coordinates were calculated, they did not satisfy this third constraint, and the largest contributions to the inequality were the differences $(b_O - b_H)^2$ and $(b_O - b_H)^2$.

The principal axis coordinates which were calculated by the methods outlined above are summarized in Table XVII. From these, bond distances and angles were computed by simple geometrical relations. These resulting molecular parameters are presented in Table XVIII. Projections of 1,3,2-dioxaborolane in the principal ab and ac planes are shown in Figure 4.

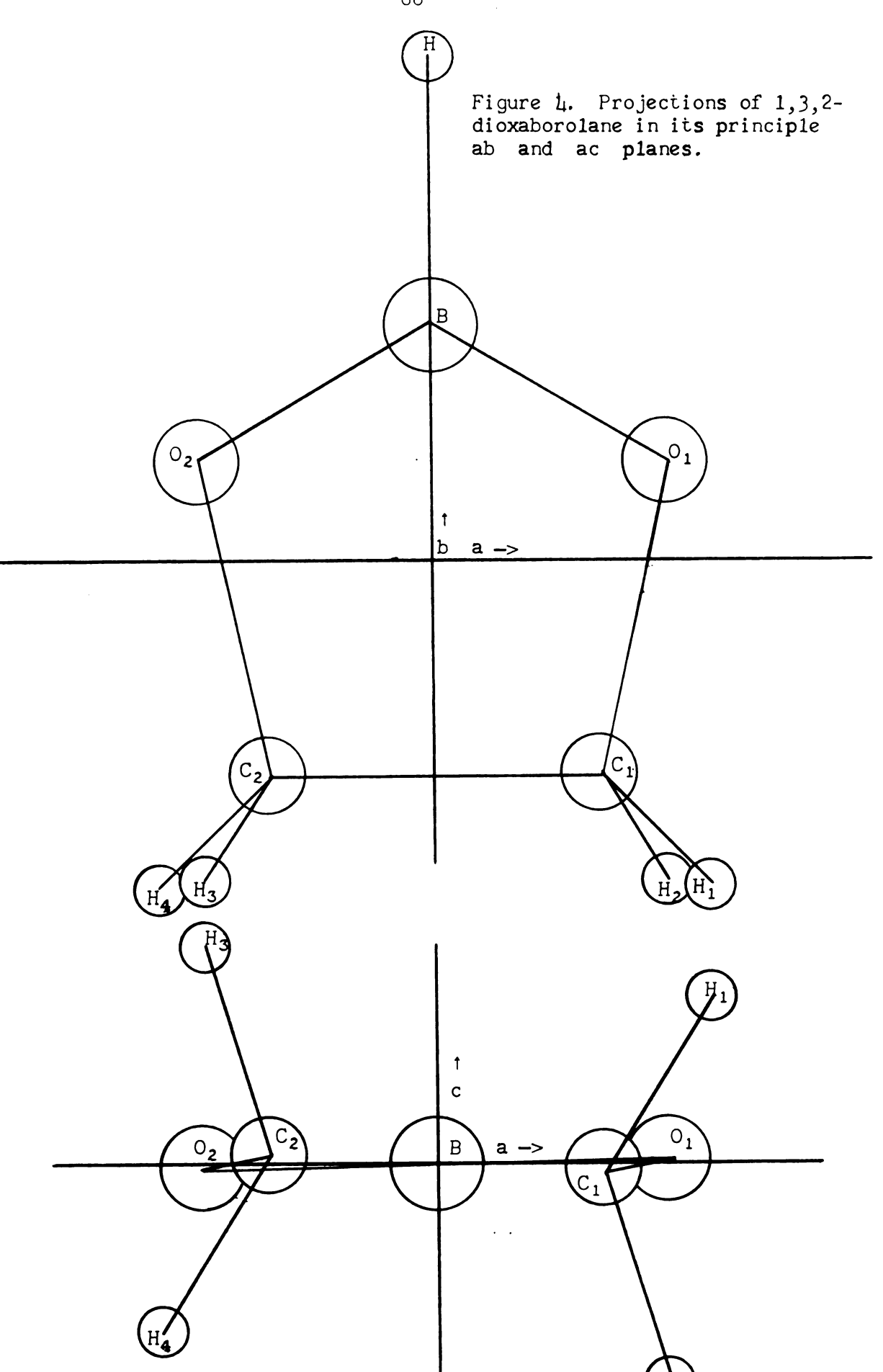
Of these parameters, only C-C may be called an r_s bond length. The rest are r_0 parameters at best. The actualy C-C substitution bond length may be slightly greater than the 1.541 Å listed; as the c coordinates are expected to be too small, due to the proximity to the ab plane. The bond length is larger than the generally accepted value 1.526 Å for simple paraffin hydrocarbons (35), but is slightly smaller than the 1.549 Å reported for trimethylene oxide. The C-H bond length is equal to the C-H_{α} distance (adjacent to the oxygen) in trimethylene oxide, and the C-H distance in methane (36). The C-O

Table XVII. Principal axis system coordinates (\mathring{A}) of the atoms in OCH_2CH_2OBH

Atom	a Coordinate	b Coordinate	c Coordinate
В	0 ^a	+1.166996	Oa
Н _В	O ^a	+2.366996 ^a	0 ^a
0	±1.147973	+0.423731	4 0.049867
С	± .767844	-0.958423	±0.062424
H ₁	±1.111590	-1.404070	7 0.999106
H ₂	±1.255828	-1.463000	±0.775078
	Ia - Iacalc	= +0.154954 AMU-A ²	
	I _b ^{exp} - I _b ^{ca1c}	= +0.000012 AMU-A ²	
	Icalc	= +0.149397 AMU-A ²	
	$\sum_{i} m_{i} a_{i} b_{i} = \sum_{i} a_{i} b_{i}$	$\sum_{i} m_{i} b_{i} c_{i} = 0$	
	$\sum_{i} m_{i} a_{i} c_{i} = 0$.404443 AMU-82	

aAssumed value.

Table XVIII. Structural parameters calculated for 1,3,2-dioxaborolane



bond length of 1.438 Å is less than the 1.449 Å determined for trimethylene oxide. The C-O bond length is in good agreement with the C-O bond length, 1.43 \pm .03 Å, determined by electron diffraction for B(OCH₃)₃ (37). The B-O bond length of 1.368 Å is in good agreement with the value 1.38 \pm .02 determined for B(OCH₃)₃. The H-C-H angle is quite close to the tetrahedral angle (109° 28') and is a degree less than the angle $H_{\alpha} - C_{\alpha} - H_{\alpha}$ (110° 18') in trimethylene oxide. The remaining bond angles (of the ring atoms) are determined to a great extent by the skeletal structure. The average angle would be 108° for a planar ring, but decreases as the ring becomes non-planar.

4.6 Interpretation of the Ring Bending Vibration

Once the molecular configuration had been established, the ring bending vibrational motion and potential function could be explored in greater detail. Any assumed model for the vibrations should be consistent with information already obtained, namely that:

- 1) there is either one low-frequency mode with two very lowlying levels, or two low-frequency modes each with a single lowlying level;
- 2) the two excited states have vibrational wave functions symmetric to a two-fold rotation about the b axis;
- 3) the vibrational frequencies decrease substantially on substituting deuteriums for the methylene hydrogens;
- 4) the rotational constants A, B and especially C increase with increasing vibrational excitation, in a non-linear fashion; and

5) the vibration-rotation interaction is similar for the parent, 4-D, and ¹³C species.

The first step was to examine the symmetry properties of the vibrational modes of 1,3,2-dioxaborolane. To simplify this examination, only the five ring atoms were considered as a first approximation. For the five-member ring with C₂^b symmetry, there are five modes which are symmetric and four which are antisymmetric to C2. Of these only two are likely to have a very low frequency of vibration. They are a symmetric and an antisymmetric out-of-plane ring deformation mode. These two modes are essentially angle bending modes, while the other seven modes contain large amounts of bond stretching. Adding the four methylene hydrogens to the ring increases the number of normal modes by six symmetric and six antisymmetric modes. Completing the structure by adding the boron hydrogen introduces one more symmetric and two more antisymmetric modes. It was felt that the modes anticipated for the bare ring would not be altered appreciably by the addition of the hydrogens. This should be a good approximation, since in most cases the normal modes which are substantially hydrogen vibrations are of high frequency and have little effect on the motions of the modes assumed in their absence.

Since (a) only one symmetric low-frequency vibrational mode was anticipated for the five-member ring model, (b) the two excited vibrational states which were observed in the spectrum seemed to lie in a series with the ground state, (c) P_{cc} increased in the series, (d) a plausible vibrational model can explain the two excited states, it was decided that the correct assignment for the two excited states was v = 1 and v = 2 for a ring deformation vibration.

The second step was to examine the qualitative nature of the potential function for the ring deformation vibration. Three facts about the potential function may be deduced from the information already presented. The first is that it must be quite anharmonic, even for low values of the vibrational quantum number. This is demonstrated by the unequal spacing between the energy levels which were estimated from the measurements of relative intensities, (E $_1$ - E $_0$ \sim 53 cm⁻¹, $E_2 - E_1 \sim 35$ cm⁻¹). The second fact is that the normal coordinate for the vibration must be symmetric to C_2^b . This has also been deduced from the relative intensities. The third fact is that there is quite probably a potential barrier at the planar configuration. This is deduced from the zig-zag variation of the rotational constants on increasing vibrational excitation. In their work on trimethylene oxide, Chan, Zinn, Fernandez, and Gwinn (13) demonstrated that a zig-zag variation of the rotational constants with v could be interpreted in terms of an equation for the single-mode vibrationrotation interaction (as equation (2-53)) to be caused by a non-linear dependence of $< Q^2 >$ on v. This zig-zag variation could be produced only by a potential function which had two minima separated by a potential barrier. The explanation for this was that superimposing a barrier on a single-minimum potential function produced the least perturbation on the energy levels whose wave functions have a node at the barrier maximum, the levels with odd values of v. Levels with even values of v were much more strongly affected, being increased in energy. At the limit of an infinite potential barrier the v = even levels had been made coincident with the next higher v = odd level, producing doubly degenerate excited states. Even if

the ground vibrational state was above the potential barrier, the presence of the barrier had an observable effect on vibrational energy levels. In fact, in the case of trimethylene oxide the barrier was calculated to lie 11 cm⁻¹ below the ground state.

In summary, then, all the effects which have been attributed to vibration-rotation interaction for 1,3,2-dioxaborolane are consistent with a double minimum potential function, and with the assignment of v = 2 to the second vibrational state.

The third step was to devise a model to describe the motion of each atom for the ring bending vibration. An indication of the type of motion present was obtained by considering the differences in the carbon atom coordinates between the ground and first excited states. The absolute values of the substitution coordinates calculated for the first excited state showed an increase of 0.011 Å in c, a decrease of 0.002 Å in b, and a decrease of 0.005 Å in a, compared to the ground state. Although far from conclusive, these indicated that the carbon atoms were moving out of the OBO plane, and that the midpoint of the C-C bond was moving closer to the boron atom. constraints were imposed on the motions in the model. First, only angle deformations were allowed, since the force constants for angle deformations are generally much smaller than for bond stretching. Second, the bond distances which had been calculated in section 4.5 were employed, and were held constant. Third, in order to locate the methylene hydrogens, they were oriented such that the HCH plane bisected the OCC angle, and the OCC plane bisected the HCH angle. The normal coordinate was taken to be ϕ , the angle between the two OCC

planes. A more convenient angle to work with was θ , the angle between the CBC and OBO planes. It was examined over the range zero degrees (a planar ring) to 30° . For each value of θ , it was possible to calculate the molecular configuration and the second moments of inertia for each of the isotopic species which had been studied.

As θ increased from 0° to 30°, the angle BOC decreased from 107.58° to 102.03°, and angle OCC decreased from 105.28° to 99.01°. The second moments of inertia, P_{aa} and P_{bb} , of each isotopic species decreased continuously and the P_{cc} increased continuously with θ ; the rotational constants A, B, C all increased with θ . There was no point at which the change in A became negative (as it had experimentally between the first and second excited vibrational states) so it must be concluded that the observed decrease ($A_2 - A_1 = -.77$ Mc/sec.) was due to the averaging over the vibrations. The vibrational averaging must also be responsible for the non-linear increase of B and C with v, since they varied smoothly with θ .

The model for the vibrational motion was employed for two further calculations. The first of these was an estimate of the effective reduced mass for the vibration in both the normal and 4-D substituted molecule. The ratio of the reduced masses could be used to interpret the differences between the normal and 4-D vibrational energies which had been deduced from the measurements of the relative intensities. The ratios of the normal and 4-D vibrational energies had been estimated to be 53:22 = 1:0.42 for the first excited states, and 88:66 = 1:0.75 for the second excited states. The reduced masses were computed as the sum of the mass of each atom times the square of the

relative distance it had moved between two values of the normal coordinate. The relative distances were normalized by dividing by the change in ϕ times its unit vector. The reduced masses calculated for $\theta = 7^{\circ}$ to $\theta = 7.5^{\circ}$ were 20.4 AMU for the normal molecule, and 30.0 AMU for the 4-D substituted molecule, a ratio of 0.68:1. Since the vibrational frequency of a harmonic oscillator varies as the -1/2 power of the reduced mass, and the frequency of a quartic oscillator varies as the -2/3 power, the estimated reduced masses are qualitatively consistent with the observed decrease of vibrational frequency from the parent to the 4-D species. Little information may be gained from a quantitative comparison, due to the large uncertainties in the estimated energy levels and in the reduced masses.

The second calculation based on the vibrational model was performed to predict the expectation value $<\theta>$ for the two excited states. To accomplish this, the angle was determined at which the calculated value of P_{cc} was equal to the experimental value, and similarly for P_{bb} . This was repeated for each vibrational state of each isotopic species for which an experimental value had been obtained. The results of these calculations are presented in Table XIX.

Although there is substantial variation in the absolute values of $<\theta>$ for each vibrational state, the differences between states is much more consistent. Using these differences and the ground state angle, $<\theta>=7.134^\circ$, which was calculated in the determination of the molecular structure, the corresponding $<\theta>$ for v=1 is predicted to be $9.94\pm.8^\circ$ and $<\theta>$ for v=2 is predicted to be $10.7\pm1^\circ$.

Table XIX. Values of < θ > (degrees) determined from the model for the vibrational motion a

- 			
		Pcc	P _{bb}
och₂ch₂obh	v = 0	7.074	8.654
	v = 1	10.632	11.109
	v = 2	11.600	11.706
QCD ₂ CD ₂ OBH	v = 0	7.479	10.735
	v = 1	10.353	12.667
	v = 2	11.214	13.145
O ¹³ CH ₂ CH ₂ OBH	v = 0	7.068	8.514
	v = 1	10.610	11.014
QCH ₂ CH ₂ O ¹⁰ ВН	v = 0	7.091	8.656

^a Value of θ for which P_{cc}^{calc} (P_{bb}^{calc}) = P_{cc}^{exp} (P_{bb}^{exp}).

4.7 Discussion

The evidence which has been presented leads to the conclusion that the potential function for the ring deformation vibration has two minima separated by a small barrier to inversion. The ground vibrational state must be higher in energy than the maximum in the potential barrier, since none of the expected effects of a tunneling inversion through the barrier were observed. Evidence for such tunneling would include anomalous Stark effects, similar to those considered for trimethylene oxide, and very large centrifugal distortion or vibration-rotation coupling perturbations, similar to those observed in cyclopentene (38). Furthermore, if the potential barrier was high compared to the lowest vibrational energy levels, a degeneracy might occur in the vibrational levels. For this case the effects of nuclear spin statistical weights on the relative intensities could not have been observed.

The interpretation of the molecular forces which produce the double minimum potential function is quite straightforward. There is obviously some strain energy present in the ring valence angles due to ring closure. The strain-free valence angle for boron is very nearly 120°, while the carbon and oxygen angles are expected to be close to the tetrahedral angle, 109° 28'. The average of these strain-free angles is 111° 34', while the angles for a planar five-member ring must average 108°. The minimum in the angle strain energy would occur at a planar configuration. Opposing the ring angle strain energy is the energy associated with the methylene hydrogen orientation. This energy is at a maximum for the eclipsed

orientation in a planar ring, and decreases with a torsion about the C-C bond. Therefore, if the methylene groups are symmetrically located with respect to the OCC planes, a small symmetric bending of the ring will produce a substantial torsion about the C-C bond, and will decrease the methylene torsional energy. It must be concluded that the potential function for the ring bending vibration is mainly due to these two opposing forces, and that the barrier at the planar configuration is not very large.

In recent years there have been a number of microwave studies of four and five-member rings, with particular interest in the questions of ring planarity and low frequency modes of vibration. outstanding example of these studies is the thorough investigation of trimethylene oxide, which has been extensively used for comparison with the results reported here for 1,3,2-dioxaborolane. For a series of four-member rings, a relation between the number of pairs of adjacent methylene groups and the relative heights of the potential barrier has been noted (39). Specifically, cyclobutane with four methylene groups is decidedly bent (40); trimethylene oxide with three methylene groups has a barrier slightly lower than the ground vibrational state; and β -propiolactone with two methylene groups has no detectable barrier (39). Most of the five member rings which have recently been studied are conjugated systems, such as furan (41) and 1,2,5-oxadiazole (42) which have no methylene groups and are planar. Cyclopentadiene is also thought to be planar (43). Cyclopentene with three methylene groups and one double bond has a high central barrier, and it has been demonstrated that there is inversion by tunneling

through the barrier (38). 1,3,2-dioxaborolane has been shown here to have a small barrier, most probably due to the two adjacent methylene groups. Since ethylene carbonate also has two adjacent methylene groups in its five-member ring, but should have much less ring angle strain (with its C=O group replacing the B-H of 1,3,2-dioxaborolane), it is predicted that a higher barrier will be present than that of 1,3,2-dioxaborolane, but lower than that of cyclopentene. The microwave spectrum of ethylene carbonate is being examined at the laboratory of Dr. James E. Boggs (44), and it will be interesting to see whether the prediction of the size of its potential barrier is correct.

V. CENTRIFUGAL DISTORTION CALCULATIONS

This chapter is concerned with centrifugal distortion, the name applied to the changes in the rigid rotor energy levels when fourth (or higher) powers of the angular momentum operators are included in the rotational Hamiltonian. The chapter begins with a summary of some well-known aspects of the theory of centrifugal distortion. Following this, at equation (5-5), some possibilities are presented for extending present methods for calculating and analyzing the effects of centrifugal distortion in molecular rotational or vibration-rotational spectra. It must be noted that the formulation of Kivelson and Wilson (45) is basic to this chapter.

The Hamiltonian for a centrifugally distorted or semi-rigid rotor is

$$H = A P_a^2 + B P_b^2 + C P_c^2 + 1/4 \sum_{\alpha} \sum_{\beta} \sum_{\gamma} \sum_{\delta} \tau_{\alpha\beta\gamma\delta} P_{\alpha}^{\rho} P_{\beta}^{\rho} P_{\gamma\delta}. \quad (5-1)$$

The 81 $\tau_{\alpha\beta\gamma\delta}$'s are the centrifugal distortion constants. Parker (46) has demonstrated that there are only 21 distinct τ 's, since in general

$$\tau_{\alpha\beta\gamma\delta} = \tau_{\gamma\delta\alpha\beta} = \tau_{\beta\alpha\gamma\delta} = \tau_{\alpha\beta\delta\gamma}$$

$$= \tau_{\beta\alpha\delta\gamma} = \tau_{\delta\gamma\alpha\beta} = \tau_{\gamma\delta\beta\alpha} = \tau_{\delta\gamma\beta\alpha} .$$
(5-2)

Further simplifications are possible in cases where the molecular system under consideration has elements of symmetry. For each of C_s , C_2 , and C_2h , a set of eight of the 21τ 's must be zero, and for the most widely studied cases of orthorhombic symmetry (C_{2_V}, V, V_h) there are only nin non-zero τ 's.

To date, centrifugal distortion has been treated by perturbation theory, usually to first order. To extend the accuracy, second-order calculations have been performed; in addition, semi-empirical P^6 terms have been added to the Hamiltonian. It was felt that these calculations might be improved by a different approach, both to obtain greater accuracy and to extend the useful range of centrifugal distortion analysis. The thought was that it would be possible to exactly diagonalize the Hamiltonian matrix for at least the orthorhombic case. These solutions would then form a convenient basis in which to calculate the perturbation energies of systems with less symmetry or with higher order $P^{\rm II}$ contributions. This diagonalization would effectively reduce by one the order of the perturbation calculation. With this goal, the study of the orthorhombic case was undertaken.

For a semi-rigid rotor with orthorhombic symmetry, there are nine non-zero τ 's, three each of the types $\tau_{\alpha\alpha\alpha\alpha},\,\tau_{\alpha\alpha\beta\beta},\,\tau_{\alpha\beta\alpha\beta}.$ When the commutation relations (equation 2-11) are applied to the operators which these τ 's multiply, terms of the type $P_{\alpha}P_{\beta}^{2}P_{\alpha}$ and $P_{\alpha}P_{\beta}P_{\alpha}P_{\beta}$ may be reduced to a combination of terms only of the type $P_{\alpha}^{2}P_{\beta}^{2}.$ If similar operators are then grouped, and the three rigid rotor terms included, the number of independent coefficients is reduced from 12 to 9. Kivelson and Wilson (45) define the new coefficients (τ') by the equations

$$B'_{X} = B_{X} + 1/4(3\tau_{YZYZ} - 2\tau_{XZXZ} - 2\tau_{XYXY}) \hbar^{4},$$

$$B'_{Y} = B_{Y} + 1/4(3\tau_{XZXZ} - 2\tau_{YZYZ} - 2\tau_{XYXY}) \hbar^{4},$$

$$B'_{Z} = B_{Z} + 1/4(3\tau_{XYXY} - 2\tau_{YZYZ} - 2\tau_{XZXZ}) \hbar^{4},$$
(5-3)

Therefore, the Hamiltonian becomes

$$H = B'_{X} P_{X}^{2} + B'_{Y} P_{Y}^{2} + B'_{Z} P_{Z}^{2} + 1/4 \{\tau'_{XXXX} P_{X}^{4} + \tau'_{YYYY} P_{Y}^{4} + \tau'_{ZZZZ} P_{Z}^{4} + \tau'_{XXYY} [P_{X}^{2}P_{Y}^{2} + P_{Y}^{2}P_{X}^{2}] + \tau'_{XXZZ} [P_{X}^{2}P_{Z}^{2} + P_{Z}^{2}P_{X}^{2}] + \tau'_{YYZZ} [P_{Y}^{2}P_{Z}^{2} + P_{Z}^{2}P_{Y}^{2}] \}.$$

$$(5-4)$$

The Hamiltonian (5-4) is the one which is to be exactly diagonalized. It is diagonal in J and M and has elements only of the type < K | K >, $< K | K \pm 2 >$, and $< K | K \pm 4 >$. It could be diagonalized directly, but some further manipulations will simplify the computation.

A new set of τ 's is defined here by the equations

$$\tau''_{XX} = 1/4 \ \tau'_{XXXX}$$
 $\tau''_{YY} = 1/4 \ \tau'_{YYYY}$
 $\tau''_{ZZ} = 1/4 \ \tau'_{ZZZZ}$ (5-5)

 $\tau''_{XY} = 1/4 \ (\tau'_{XXYY} - 1/2 \ \tau'_{XXXX} - 1/2 \ \tau'_{YYYY})$
 $\tau''_{XZ} = 1/4 \ (\tau'_{XXZZ} - 1/2 \ \tau'_{XXXX} - 1/2 \ \tau'_{ZZZZ})$
 $\tau''_{YZ} = 1/4 \ (\tau'_{YYZZ} - 1/2 \ \tau'_{YYYY} - 1/2 \ \tau'_{ZZZZ})$.

Then by noting that

$$P_X^4 + P_X^2 P_Y^2 + P_X^2 P_Z^2 = P_X^2 [P_X^2 + P_Y^2 + P_Z^2] = P_X^2 P^2$$
, (5-6)

and similarly for y and z, equation 5-4 may be re-written as

$$H = B_{X}' P_{X}^{2} + B_{Y}' P_{Y}^{2} + B_{Z}' P_{Z}^{2} + T''_{XX} P^{2} P_{X}^{2} + T''_{YY} P^{2} P_{Y}^{2} + T''_{ZZ} P^{2} P_{Z}^{2} + T''_{XX} [P_{X}^{2} P_{Y}^{2} + P_{Y}^{2} P_{X}^{2}] + T''_{XZ} [P_{X}^{2} P_{Z}^{2} + P_{Z}^{2} P_{X}^{2}] + T''_{YZ} [P_{Y}^{2} P_{Z}^{2} + P_{Z}^{2} P_{Y}^{2}]$$

$$(5-7)$$

This form of the Hamiltonian may be factored into five separate parts to facilitate the diagonalization. The basis set in which the elements are calculated has been assumed to be the same as was used in section 2.2, including the Wang transformation, $\widetilde{X}HX$. The Hamiltonian is

$$H = H^{(0)} + H^{(1)} + H^{(2)} + H^{(3)} + H^{(4)}$$
 (5-8)

where

$$H^{(0)} = 1/2 (B_X' + B_Y')P^2$$
 (5-9)

is diagonal, and constant in the quantum number K;

$$H^{(1)} = 1/2[2B_Z' - B_X' - B_Y'][P_Z^2 + b(P_X^2 - P_Y^2)], (5-10)$$

where

$$b = \frac{B_{X}' - B_{Y}'}{2B_{Z}' - B_{X}' - B_{Y}'}.$$

 $H^{(1)}$ is in Wang's reduced energy form, and has elements < $K \mid K >$ and < $K \mid K \pm 2 >$. Furthermore,

$$H^{(2)} = 1/2(\tau''_{XX} + \tau''_{YY})P^{4}$$
 (5-11)

is diagonal, and also constant in K;

$$H^{(3)} = 1/2 P^{2} [2\tau''_{ZZ} - \tau''_{XX} - \tau''_{YY}] [P_{Z}^{2} + f_{\tau} (P_{X}^{2} - P_{Y}^{2})]$$
 (5-12)

is a reduced distortion energy similar to $H^{(1)}$, with $\langle K | K \rangle$ and $\langle K | K \rangle$ elements, and with

$$f_{\tau} = \frac{\tau''_{XX} - \tau''_{YY}}{2\tau''_{ZZ} - \tau''_{XX} - \tau''_{YY}}.$$

Finally,

$$H^{(4)} = \tau''_{XY}[P_X^2 P_Y^2 + P_Y^2 P_X^2] + \tau''_{XZ}[P_X^2 P_Z^2 + P_Z^2 P_X^2] + \tau''_{YZ}[P_Y^2 P_Z^2 + P_Z^2 P_Y^2], \text{ and}$$
(5-13)

has $\langle K | K \rangle$, $\langle K | K \pm 2 \rangle$, $\langle K | K \pm 4 \rangle$ elements.

The blocks of (5-8) in the Wang symmetric rotor basis are symmetric across the principal diagonal and have the form

$$E^{+} = \begin{pmatrix} E_{00} & \sqrt{2}E_{02} & \sqrt{2}E_{04} & 0 & 0 \\ \sqrt{2}E_{02} & E_{22} + E_{2-2} & E_{24} & E_{26} & 0 \\ \sqrt{2}E_{04} & E_{24} & E_{44} & E_{46} & E_{66} \\ \end{pmatrix}$$

$$O^{+} = \begin{pmatrix} E_{11} + E_{1-1} & E_{13} + E_{1-3} & E_{15} & O & O \\ E_{13} + E_{1-3} & E_{33} & E_{35} & E_{37} & O \\ E_{15} & E_{35} & E_{55} & E_{57} & E_{77} \end{pmatrix}$$
(5-14)

 $E^- = E^+$ Except/the first row and column are omitted and $E_{22} + E_{2-2}$ is replaced by $E_{22} - E_{2-2}$.

 $O^- = O^+$ Except that the (1,1), (1,2), (2,1) terms are now $E_{11} - E_{1-1}$, $E_{13} - E_{1-3}$, $E_{13} - E_{1-3}$ respectively.

The K dependent elements of $H' = H^{(1)} + H^{(3)} + H^{(4)}$ are

$$< K | H' | K > = 1/2 K^{2} [2B_{Z}' - B_{X}' - B_{Y}' + P^{2} (2\tau''_{ZZ} - \tau''_{XX} - \tau''_{YY})$$
 $+ \tau''_{XY} \{ (P^{2} - K^{2}) (P^{2} - K^{2} + 2) + 3K^{2} \}$
 $+ 2(\tau''_{YZ} + \tau''_{XZ}) (P^{2} - K^{2}) \},$

In this form, the semi-rigid rotor should be relatively easy to diagonalize. The detailed method to be used will depend on the considerations of computer efficiency and timing, the size of the submatrices to be diagonalized, and the ease of coding the procedure. It should prove useful to take advantage of the continued fraction program which is presently available (Appendix B). The < K | K \pm 4 > elements could be treated by Givens' method (47) to reduce the matrix to tri-diagonal form, and the diagonalization completed with the continued fraction method. This method would also allow computation of the rigid rotor eigenvalues for comparison purposes.

Once the eigenvalues and eigenvectors of (5-8) have been obtained, they may be used to calculate first and higher order perturbation energy contributions from distortion constants admitted by lower symmetry or from higher powers of Pⁿ.

A second use would be to check the accuracy of results which have been obtained by perturbation theory using the rigid rotor as the zero order problem. Such a comparison could be made, for example, with the results of Pierce, DiCianni and Jackson for OF_2 (48).

BIBLIOGRAPHY

- 1. Cleeton, C. E. and N. H. Williams, Phys. Rev. 45, 234 (1934).
- 2. a. Bleaney B. and R. P. Penrose, Nature 157, 339 (1946).
 - b. Bleaney B. and R. P. Penrose, Phys. Rev. 70, 775 (1946).
- 3. a. Coles, D. K. and W. E. Good, Phys. Rev. 70, 979 (1946).
 - b. Good, W. E., Phys. Rev. 70, 213 (1946).
- 4. Dailey, B. P., R. L. Kyhl, M. W. P. Strandberg, J. H. Van Vleck and E. B. Wilson, Jr., Phys. Rev. 70, 984 (1946).
- 5. Burkhard, D. G. and D. M. Dennison, Phys. Rev. 84, 408 (1951).
- 6. a. Herschbach, D. R., Thesis, Harvard University, 1958.
 - b. Herschbach, D. R., J. Chem. Phys. 31, 91 (1959).
 - c. Lin, C. C. and J. D. Swalen, Revs. Mod. Phys. 31, 841 (1959).
- 7. Dakin, T. W., W. E. Good, and D. K. Coles, Phys. Rev. <u>70</u>, 560 (1946).
- 8. Hughes, R. H. and E. B. Wilson, Jr., Phys. Rev. 71, 562 (1947).
- 9. Debye, P. J. W., Polar Molecules, Chemical Catalog Co., New York, (1929).
- 10. Shulman, R. G. and C. H. Townes, Phys. Rev. 77, 500 (1950).
- 11. Kraitchman, J., Am. J. Phys. 21, 17 (1953).
- 12. Costain, C. C., J. Chem. Phys. 29, 864 (1958).
- 13. Chan, S. I., J. Zinn, J. Ferandez, and W. D. Gwinn, J. Chem. Phys. 33, 1643 (1960); Chan, S. I., J. Zinn, and W. D. Gwinn, J. Chem. Phys. 34, 1319 (1961).
- 14. Schlesinger, H. I. and A. B. Burg, Chem. Rev. 31, 1 (1942).
- 15. Rose, S. H. and S. G. Shore, Inorg. Chem. 1, 744 (1962).
- 16. Wang, S. C., Phys. Rev. <u>34</u>, 243 (1929).
- 17. Ray, B. S., Zeits. F. Physik <u>78</u>, 74 (1932).

- 18. King, G. W., R. M. Hainer, and P. C. Cross, J. Chem. Phys. <u>11</u>, 27 (1943).
- 19. Golden, S. and E. B. Wilson, Jr., J. Chem. Phys. 7, 869 (1948).
- 20. Casimir, H. B. G., On the Interaction Between Atomic Nuclei and Electrons, Teylers Tweeke Genootschap, E. F. Bohn, Haarlem (1936).
- 21. Bragg, J. K. and S. Golden, Phys. Rev. 75, 735 (1949).
- 22. Townes, C. H. and B. P. Dailey, J. Chem. Phys. 17, 782 (1949).
- 23. Eckart, C., Phys. Rev. 47, 552 (1935).
- 24. Herschback, D. R. and V. W. Laurie, J. Chem. Phys. 37, 1668 (1962).
- 25. Oka, T. and Y. Morino, J. Mol. Spec. 6, 472 (1961).
- 26. Herschbach, D. R. and V. W. Laurie, J. Chem. Phys. 40, 3142 (1964).
- 27. Douglas, A. E. and C. K. Møller, J. Chem. Phys. 22, 275 (1954).
- 28. a. Cox, J. D., H. S. Turner and R. J. Warne, J. Chem. Soc., 3167 (1950); as reported (page 35) in,
 - b. Murry, A. and D. L. Williams, Organic Syntheses with Isotopes, Interscience, New York, 1958.
- 29. Cox, J. D. and H. S. Turner, J. Chem. Soc., 3176 (1950); as reported in reference 28-b, page 905.
- 30. Popplewell, D. S. and R. G. Wilkings, J. Chem. Soc., 2521 (1955); as reported in reference 28-b, page 495.
- 31. Townes, C. H. and A. L. Schawlow, <u>Microwave Spectroscopy</u>, McGraw-Hill, New York (1955).
- 32. Shore, S. G., private communication.
- 33. Wilson, E. B., Jr., J. C. Decius and P. C. Cross, Molecular Vibrations, McGraw-Hill, New York (1955), page 147 ff.
- 34. Marshall, S. A. and J. Weber, Phys. Rev. 105, 1502 (1957).
- 35. Lide, D. R., Jr., J. Chem. Phys. <u>33</u>, 1519 (1960).
- 36. Sheperd, G. G. and H. L. Welsh, J. Mol. Spec. $\underline{1}$, 277 (1957).
- 37. Bauer, S. H. and J. T. Beach, J. Am. Chem. Soc. 63, 1394 (1941).

- 38. a. Rathjens, G. W., Jr., J. Chem. Phys. <u>36</u>, 2401 (1962).
 - b. Butcher, S. S. and C. C. Costain, J. Mol. Spec. 15, 40 (1965).
- 39. Boone, D. W., C. O. Britt and J. E. Boggs, (to be published).
- 40. Dunitz, J. D., and V. Schomaker, J. Chem. Phys. 20, 1703 (1952).
- 41. Bak, B., D. Christensen, W. B. Dixon, L. Hansen-Nygaard, J. Pastrup-Andersen, and M. Schöttlander, J. Mol. Spec. 9, 124 (1962).
- 42. Cox, A. P. and E. Saegebarth, (to be published).
- 43. Laurie, V. W., J. Chem. Phys. 24, 635 (1956).
- 44. Boggs, J. E., Private communication.
- 45. Kivelson, D. and E. B. Wilson, Jr., J. Chem. Phys. 20, 1575 (1952).
- 46. Parker, P. M., J. Chem. Phys. 37, 1596 (1962).
- 47. Givens, W., Assoc. Comp. Mach. 4, 298 (1957).
- 48. Pierce, L., N. DiCianni, and R. H. Jackson, J. Chem. Phys. 38, 730 (1963).
- 49. Swalen, J. D. and L. Pierce, J. Math. Phys. 2, 736 (1961).
- 50. Schwendeman, R. H., J. Mol. Spec. 7, 280 (1961).

APPENDICES

APPENDIX A

COMPUTER PROGRAM "EIGVALS"

This program calculates rotational energy eigenvalues, quadrupole coupling energies, transition frequencies, line strengths, and Stark effect coefficients for a rigid asymmetric rotor. It was originally coded in FORTRAN-60 and has been modified to run in 3600 FORTRAN for the Control Data 3600 computer at Michigan State University.

The heart of the program is the routine for diagonalizing the reduced energy Hamiltonian. The reduced energy matrix is established in the computer from the values of the rotational constants which are read in as input data. The matrix elements are those appropriate to the III^1 or I^r axis identification, depending on whether the rotational constants correspond more closely to an oblate or to a prolate rotor. The diagonalization utilizes a continued fraction calculation with a Newton-Raphson second-order iterative procedure as suggested by Swalen and Pierce (49). The "best development" algorithm of Swalen and Pierce is also used, with good results. It has been found that it is possible to speed convergence and eliminate the possibility of convergence to an incorrect root, by employing an additional algorithm to obtain the required initial estimate of each eigenvalue. The linear and quadratic solutions for the low J matrix blocks are calculated directly. It is then possible to extrapolate the eigenvalues to initially estimate higher J eigenvalues. The extrapolation is approximately of the order (J - 2|K|) in the successive differences of the eigenvalues which have already been computed.

The extrapolation improves the initial estimates, especially for high J, low K eigenvalues, which are precisely the ones which have the greatest deviation from the linear extrapolation which has often been used previously. The final eigenvalue of each matrix block is estimated from the criterion of invariance of the trace for the transformation.

The eigenvectors are then used to compute the average values of P_z^2 (i.e. $< P_z^2>$) from which $< P_x^2>$ and $< P_y^2>$ are then calculated. These have been shown to be also the partial derivatives of the energy with respect to the rotational constants. The quadrupole coupling constant coefficients α_q and β_q (equation 2-38) are calculated from the derivatives, and the energies W_Q are obtained by multiplying by the values of χ_{aa} and χ_{bb} - χ_{cc} which were read into the computer as input data.

The final section of the program was written by Dr. Schwendeman. The line strength for each possible transition is calculated by transforming the appropriate direction cosine matrix element (50) with the eigenvectors previously computed. Only the transitions which have a frequency between 8,000 and 40,000 Mc/sec. and a relative line strength greater than 0.1 are printed out. Finally the Stark coefficients are computed by second-order perturbation from the direction cosine matrix elements and the energy levels.

APPENDIX B

KRAITCHMAN-TYPE EQUATIONS FOR THE 4-D SUBSTITUTION

The substitution of four deuterium atoms for the four methylene hydrogen atoms in 1,3,2-dioxaborolane produces the following changes in the values of the second moments of inertia:

$$P_{XX}^{!} = P_{XX} + \Delta m(x_{1}^{2} + x_{2}^{2} + x_{3}^{2} + x_{4}^{2}) - \frac{\left[\Delta m(x_{1} + x_{2} + x_{3} + x_{4})\right]^{2}}{M + 4\Delta m} \text{ etc.}$$

$$P_{XY}^{!} = \Delta m(x_{1}y_{1} + x_{2}y_{2} + x_{3}y_{3} + x_{4}y_{4}) - \frac{\Delta m^{2}}{M + 4\Delta m}[(x_{1} + x_{2} + x_{3} + x_{4})(y_{1} + y_{2} + y_{3} + y_{4})] \text{ etc.}$$
(B-1)

where

$$\Delta m = m_D - m_H$$

M = parent molecular weight, and

 $(x_1,\ x_2,\ \cdots,\ z_4)$ are the coordinates of the hydrogens in the parent axis system.

The elements in (B-1) may be simplified by satisfying the requirement of C_2^y symmetry;

$$x_1 = -x_3, \quad x_2 = -x_4,$$

 $y_1 = y_3, \quad y_2 = y_4,$
 $z_1 = -z_3, \quad z_2 = -z_4.$ (B-2)

These reduce the elements of (B-1) to

$$P_{xx}' = P_{xx} + 2\Delta m(x_1^2 + x_2^2),$$

$$P_{yy}' = P_{yy} + \frac{2\Delta m}{M + 4\Delta m}[M(y_1^2 + y_2^2) + 2\Delta m(y_1 - y_2)^2],$$

$$P_{zz}' = P_{zz} + 2\Delta m(z_1^2 + z_2^2),$$

$$(B-3)$$

$$P_{xy} = 0,$$
 $P_{yz} = 0, \text{ and}$
 $P_{xz} = 2\Delta m(x_1z_1 + x_2z_2).$

The experimental second moments $P_{XX}^{"}$, $P_{YY}^{"}$, $P_{ZZ}^{"}$ are the roots of the determinant |P'| = 0. $P_{YY}^{"}$ is already a root, therefore,

$$P_{yy}'' - P_{yy} = \frac{2\Delta m}{M + 4\Delta m} \left[M(y_1^2 + y_2^2) + 2\Delta m(y_1 - y_2)^2 \right].$$
 (B-4)

 $P_{xx}^{"}$ and $P_{zz}^{"}$ are the roots of the remaining 2 x 2 determinant

$$\begin{vmatrix}
P'_{xx} - P'' & P'_{xz} \\
P'_{xz} & P'_{zz} - P'' \\
\end{vmatrix} = 0 \qquad (B-5)$$

Expanding the determinant and equating the resulting coefficients of $(P'')^1$ and $(P'')^0$ to P''_{xx} + P''_{zz} and $P''_{xx}P''_{zz}$, leads to the two final equations,

$$P_{XX}^{"}P_{ZZ}^{"} - P_{XX}P_{ZZ} = 2\Delta m[P_{ZZ}(x_1^2 + x_2^2) + P_{XX}(z_1^2 + z_2^2) + 2\Delta m(x_1z_2 - x_2z_1)^2] \text{ and}$$

$$(P_{XX}^{"} - P_{XX}) + (P_{ZZ}^{"} - P_{ZZ}) = 2\Delta m[x_1^2 + x_2^2 + z_1^2 + z_2^2].$$

These three equations (B-4), (B-5), (B-6), can not be reduced to simple expressions in the coordinates of one atom. They were, however, used in this form with other equations as reported in section 4.5 to determine the coordinates of the methylene hydrogens.

